PV-ARRAY GRID-CONNECTED THREE-PHASE INVERTER CONTROLLED BY MODEL PREDICTIVE CONTROLLER

2022
MASTER THESIS
ELECTRICAL-ELECTRONICS ENGINEERING

Aadil Salam Ahmed ABUMLEH

Thesis Advisor
Assist. Prof. Dr. Ozan GÜLBUDAK

PV-ARRAY GRID-CONNECTED THREE-PHASE INVERTER CONTROLLED BY MODEL PREDICTIVE CONTROLLER

Aadil Salam Ahmed ABUMLEH

Thesis Advisor
Assist. Prof. Dr. Ozan GÜLBUDAK

T.C.
Karabük University
Institute of Graduate Programs
Department of Electrical-Electronics Engineering
Prepared as a
Master Thesis

KARABÜK
November 2022

I certify that in my opinion the thesis “PV-ARRAY GRID-CONNECTED THREE-PHASE INVERTER CONTROLLED BY MODEL PREDICTIVE CONTROLLER” submitted by Aadil Salam Ahmed ABUMLEH is fully adequate in scope and in quality as a thesis for the degree of Master of Science.

Assist. Prof. Dr. Ozan GÜLBUDAK .....
Thesis Advisor, Department of Electric and Electronics

This thesis is accepted by the examining committee with a unanimous vote in the Department of Electrical-Electronics Engineering as a Master of Science thesis. 25/11/ 2022

Examining Committee Members (Institutions)		Signature
Chairman	: Assist. Prof. Dr. Ozan GÜLBUDAK (KBU)	.....
Member	: Assist. Prof. Dr. Mustafa GÖKDAĞ (KBU)	.....
Member	: Assoc. Prof. Dr. Osman ÇİÇEK (KU)	.....

The degree of Master of Science by the thesis submitted is approved by the Administrative Board of the Institute of Graduate Programs, Karabük University.

Assoc. Prof. Dr. Müslüm KUZU .....
Director of the Institute of Graduate Programs

"I declare that all the information within this thesis has been gathered and presented in accordance with academic regulations and ethical principles and I have according to the requirements of these regulations and principles cited all those which do not originate in this work as well."

Aadil Salam Ahmed ABUMLEH

ABSTRACT

M. Sc. Thesis

PV-ARRAY GRID-CONNECTED THREE-PHASE INVERTER CONTROLLED BY MODEL PREDICTIVE CONTROLLER

Aadil Salam Ahmed ABUMLEH

Karabük University
Institute of Graduate Programs
The Department Electrical

Thesis Advisor;
Assist. Prof. Dr. Ozan GÜLBUDAK
November 2022, 66 pages

The PV-Array grid connected inverter is a promising solution to the growing demand for energy, very good combined with modern live needs specification, offers a solution to urgent problem the humanity facing like pollution and global warming in addition it is feasible, economic almost maintenance free and socio-economic benefits. This work is present a three-phase inverter connected with PV-Array using maximum power point tracking (MPPT) algorithm, the inverter controlled by MPC controller to inject pure power into the grid when the generated power exceeds the local load and in stand-alone mode the redundant power (generated by the PV-Array system) store in the batteries.

Key words **:** PV-Array, inverter, MPC controller, climate change, stand-alone mode, batteries.

Science Code :90526

ÖZET

Yüksek Lisans Tezi

MODEL TAHMIN DENETLEYICISI TARAFINDAN KONTROL EDILEN PV DIZI IZGARAYA BAĞLI ÜÇ FAZLI INVERTÖR

Aadil Salam Ahmed ABUMLEH

Karabük Üniversitesi
Lisansüstü Eğitim Enstitüsü
Elektrik Bölümü

Tez Danışmanı
Dr. Öğr. Üyesi Ozan GÜLBUDAK
Kasım 2022, 66 sayfa

PV-Array şebekeye bağlı invertör, artan enerji talebine umut verici bir çözümdür, modern canlı ihtiyaç spesifikasyonu ile birlikte çok iyidir, insanlığın kirlilik ve küresel ısınma gibi karşılaştığı acil soruna bir çözüm sunar, ayrıca uygulanabilir, ekonomik neredeyse bakım gerektirmez ve sosyo-ekonomik faydalardır. Bu çalışma, maksimum güç noktası izleme (MPPT) algoritması kullanılarak PV Dizisine bağlı üç fazlı bir invertör, üretilen güç yerel yükü aştığında şebekeye saf güç enjekte etmek için MPC denetleyicisi tarafından kontrol edilen invertör ve bağımsız modda yedek gücü (PV-Array sistemi tarafından üretilen) pillerde depolanır.

Anahtar kelimeler: PV Dizisi, invertör, MPC kontrolörü, iklim değişikliği, bağımsız mod, piller.

Biilim Kodu :90526

ACKNOWLEDGMENT

First, I would like to give thanks to my advisor, Assist. Prof. Dr. Ozan GULBUDAK, for his great interest and assistance in preparing this thesis.

TABLE OF CONTENTS

Page

Page

LIST OF FIGURES

Page

Page

Page

LIST OF TABLES

Page

SYMBOLS AND ABBREVITIONS INDEX

SYMBOLS

α-β	: Clarke transformation for three phase system
ξ	: vector symbol
$K\alpha\beta$	: Clarke transformation matrix
$Kabc$	: the opposite to Clarke transformation matrix
Φ	: the solution of state space matrix (A) in discrete time domain
Γ	: the solution of discrete space matrix (B) in discrete time domain
λ	: the converting factor of discrete integration

ABBRAVIATIONS

MPPT	: Maximum Power Point Tracking
IC	: Integrated Circuit
CO2	: Carbon Dioxide
CH4	: Methane
PWM	: Pulse Width Modulation
PR	: Proportional Resonant Controller
PID	: Proportional Integration Derivative Controller
MPC	: Model Predictive Controller
LC-filter	: Inductance Capacitor Filter
LCL-filter	: Inductance Capacitor Inductance Filter
FCS	: Finite Control Set
ESS	: Energy Storage System
RE	: Renewable Energy
THD	: total harmonic distortion
VSI	: voltage source inverter
PLL	: phase locker loop

PSO	: practical swarm optimization
Kp, Ki and Kd	: proportional , integral and derivative gain of PID controller
CSC	: current source converter
LVRT	: low voltage riding through
FCS-MPC	: finite control set model predictive controller
DC	: direct current
AC	: alternative current
FCS-MPCC	: finite control set of model predictive current controller
PI	: proportional integration controller
IC-MPC	: incremental conductance model predictive controller
VOC	: voltage oriented control
SMC	: sliding model controller
CCS-MPC	: continues control set model predictive controller
W1	: first resonance frequency of LCL filter
W2	: second resonance frequency of LCL filter
L	: filter inductance
C	: filter capacitor
PDPC	: predictive direct power control
MOSFET-diode	: metal oxide semiconductor field effected transistor
x(K)	: the discrete state space of the system
y(K)	: the discrete output of the system
ZOH	: the zero order hold
x(t)	: the state space of the system (time domain)
A	: state space matrix
B	: input state space matrix
X(s)	: Laplace transform of state space matrix
x(kh)	: discrete state space matrix
y(kh)	: discrete output state space matrix
Vg	: voltage of inverter side
Vs	: voltage of grid side
Vc	: voltage of the LCL-filter capacitor
if	: filter input current
is	: grid injected current

L1,L2 and C	: the inductance and capacitor of the LCL-filter
g	: the cost function symbols
$imeas$	: the measured current
$iref$	: reference current
$i\alpha(k+1)ref$	: discrete Clarke transformation of reference current
$i\beta(k+1)$	: discrete Clarke transformation of reference current
$iap(k+1)$	: predicted discrete Clarke transformation of reference current
$i\beta p(k+1)ref$	: predicted discrete Clarke transformation of reference current
$ia(k+1)ref$	: phase A of three phase system reference current
$iap(k+1)$	: predicted phase A of three phase system reference current
$ib(k+1)ref$	: phase B of three phase system reference current
$ibp(k+1)$	: predicted phase B of three phase system reference current
$ic(k+1)ref$	: phase C of three phase system reference current
$icp(k+1)$	: predicted phase C of three phase system reference current
Sa, Sb, and Sc	: is the switching state of the inverter
$VaN, VbN\ and\ VcN$	: is the DC input voltage on inverter side

PART 1

INTRODUCTION

1.1. BACKGROUND OF FOSSIL FUEL AND RENEWABLE ENERGY

When the first human discovered fire for the first time, it was – and still is – a fascinating and valuable tool to this day. The first human used it as a source of light and heat, and it is still a primary power source to this day.

Before the Industrial Revolution, we used human and animal muscle to do the work. However, after 1785, the Industrial Era began, and engines fueled by coal started to do hard work. Then the Electricity Age started in the nineteenth century with the commercial availability of electricity, especially with the invention of the commercial induction motor at that time. The seeds of the age of modern solid-state electronics began with the design and production of the transistor in 1948. After that, the thyristor was introduced in 1958, and the age of the solid-state power electronic began, followed by the invention of integrated circuits (IC), and later of robots. Now we are living in the Internet era (which makes the whole world a small town) [1].

Today, electricity is the primary source of energy because it is flexible, easy to control, easy to generate and transmit. Other kinds of energy (fire (heat), kinetic, radiation, nuclear, etc.) is used to produce electricity, but increases in population with higher living standards leads to increases in electricity standards and energy demand at a rate of approximately 2.6% per year until 2040 [2].

The primary source for the generation of electricity is fossil fuel (oil, coal and natural gas), the leading fuel for these electricity generation plants [3], as shown below in Figure 1.1.

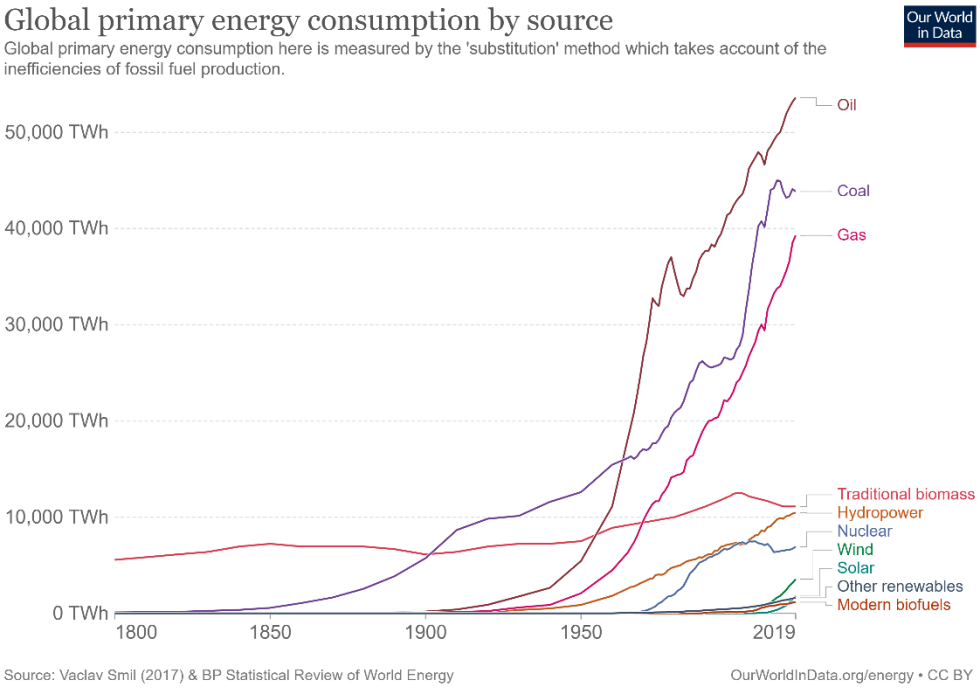

Figure 1.1. Primary energy consumption [3].

Due to global warming and a large number of greenhouse emissions (such as CO_2, CH_4, etc.) as shown in Figure 1.2, environmental and health problems will inevitably increase.

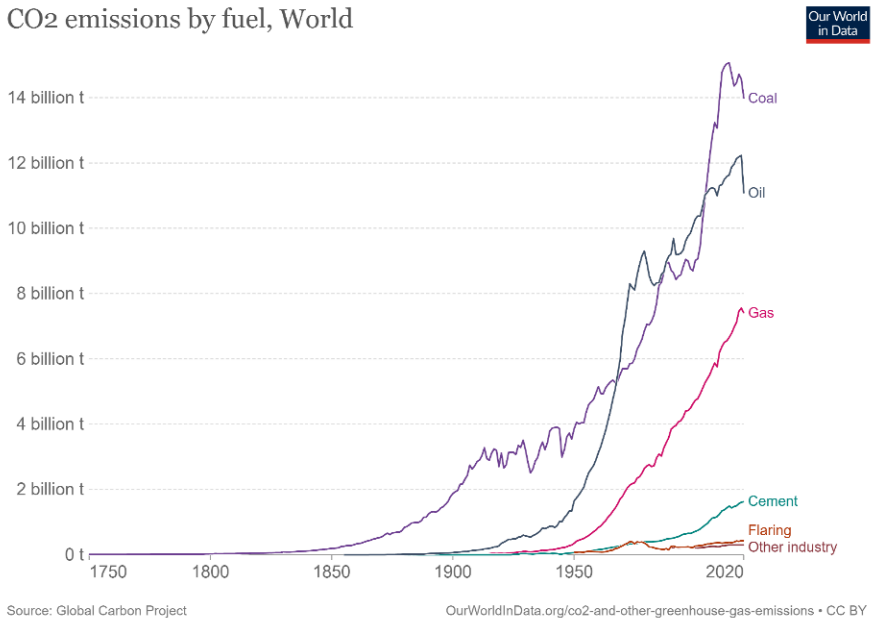

Figure 1.2. CO_2 emission for different kinds of fossil fuel [3].

Green energy sources offer an excellent alternative to fossil fuels from more than one aspect.

1.1.1. Advantages of Renewable Energy

- It is environmentally friendly and does not emit CO_2 or any greenhouse gases.
- It does not require a large area of land on which to operate as is the case with conventional fossil fuel electricity generation plants. Green energy sources are simple and do not need additional refining sources as do fossil fuels, as can be seen in Figure 1.3.

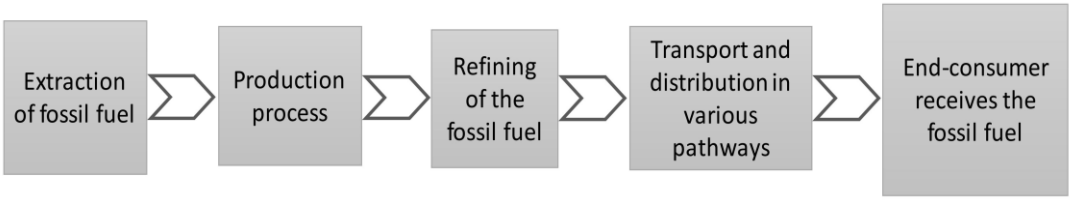

Figure 1.3. Stages of fossil fuel production [4].

Green energy sources can overcome this complex, expensive and environmentally harmful process.

- Fossil fuel sources are not able to be replenished due to the high rate of fuel extraction. Many fossil fuel reservoirs will be depleted in the future (Figure 1.4).

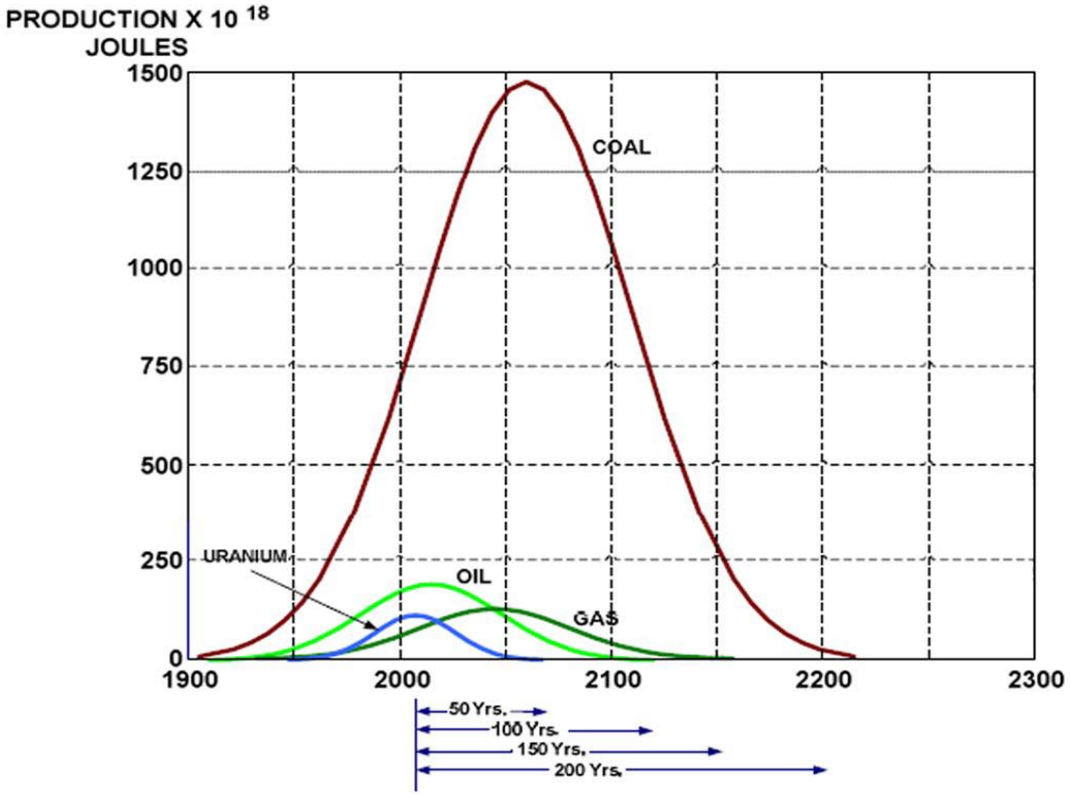

Figure 1.4. Fossil fuel depletion [1].

- The fossil fuel industry has been developed and refined for more than a century, so it requires a substantial investment to bring about improvements while many of the renewable sources are in the innovation process. Therefore, small investments will bring significant productivity gains and significant improvements.
- The traditional manner of producing electricity (giant bulky planets) needs a large area for installation, while renewable energy can be installed almost anywhere, such as on the roofs of houses or buildings.
- Traditional electricity generation requires large electricity infrastructure (transmission lines, protection devices and other grid facilities) to transfer the energy to consumers. In contrast, renewable energy can be installed near the consumer, so in many cases, it overcomes this problem considering that one-third of the world population lives outside the electric grid, thereby making renewable energy very attractive [1].

- Traditional energy generation plants require expensive maintenance while renewable energy, in many cases, is almost maintenance free such as PV-arrays.
- The central topology of traditional electricity generation consists of three stages (generation, transmission and distribution), making it vulnerable because if a fault occurs in any of these rings, it will disturb the energy delivered to the consumer. On the other hand, renewable energy connects directly to the consumer and does not need more than one stage in most cases.
- Power flow in traditional electricity generation is in one direction. There is no direct connection between the consumer and the generation stage. However, this is not the case with renewable energy, especially if combined with communication networks such as small or micro grids. In the flow of the power, information is in two directions, and load management and storage in such cases become very effective (demand-side energy management) [1].
- The rapid increase in fossil fuel prices and at the same time, rapid decreases in renewable energy system prices, especially the costs of PV-Array or solar cells, makes it an attractive alternative to fossil fuels.
- Many countries around the world do not have indigenous energy sources, including developed countries such as Japan, which uses nuclear power as an alternative to fossil fuels. However, the last disaster of the Fukushima-Daiichi nuclear reactors shifted the focus toward renewable energy as an alternative to atomic sources.

1.1.2. Disadvantages of Renewable Energy

- One significant disadvantage is that renewable energy is intermittent, such as the sun for solar energy or wind for air turbines.
- Harmonics are usually higher for renewable energy sources than for traditional sources [5], as shown in Figure 1.5.

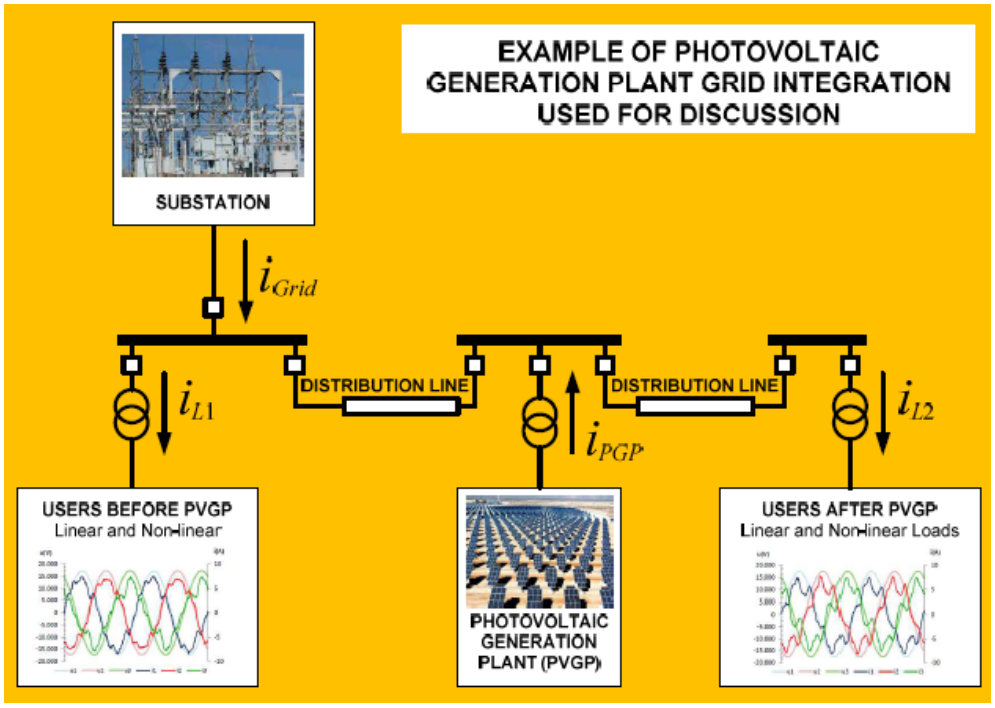

Figure 1.5. Effect of connecting PVGP with the grid and harmonic effects [5].

- In some countries, electricity generated from coal is cheaper than electricity generated from renewable energy plants. However, with time economic benefits will accumulate, as shown in Figure 1.6. Renewable energy sources will overcome initial installation costs over time. However, this does not change the fact that they initially have high installation costs [2].

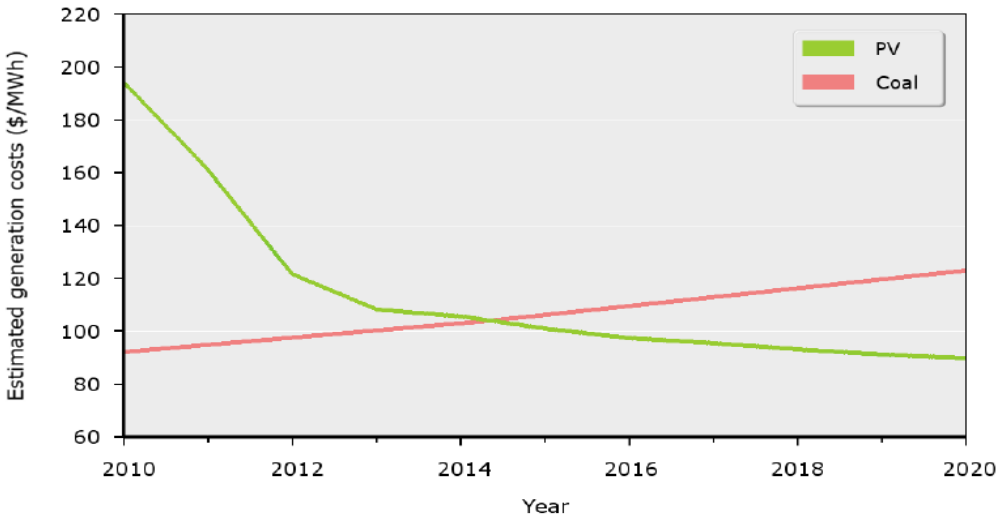

Figure 1.6. Estimated amount of electricity generated from coal and renewable energy in South Africa [2].

- Withdrawal is the conventional way to generate energy. A rotating mass (rotor) coupling provides inherent inertia and torque that mitigates multiple undesired events in the power system, such as rapid frequency changes, slight power imbalances, and high-frequency oscillations, which is not the case with renewable energy sources. However, the dynamic response of an inverter is ultra-high speed in comparison to the traditional mechanical way of generating energy. However, at the same time, when many more renewable energy sources connect to the grid with smaller numbers of synchronous machines (with mechanical rotating mass), it makes the system more vulnerable to stability issues [6].

1.2. RENEWABLE ENERGY

According to the above comparison of fossil fuel energy sources and renewable energy sources, the latter is the logical choice or the only alternative to fossil fuels due to the looming environmental crisis (the largest parts of many countries around the world will be submerged below sea level if global warming continues at the current rate). Around 50% of Bangladesh will be underwater in the next 300 years and according to the UN, Indian agriculture will decrease by 38% around 2080 due to drought [1].

1.2.1. Power Electronics

In the middle of the twentieth century, the discovery of the solid-state transistor was a great leap for humanity (firs invented in 1948 followed by the thyristor in commercial form in 1958). After that, development of solid-state circuits such as ICs, microprocessors continued. Solar cell installation is accelerating around the world, which draws more attention and investment in power electronics and green energy sources as well as the rapid reduction of prices, leading to further development.

the rapid development in power electronics has enhanced the control and saving of power by almost 70% in some countries. Soon this saving will be 100%; therefore, almost all power will pass through power electronic devices, which will optimize the performance, control and saving of electric power [1, 7].

1.2.2. Control Methods

The rapid development of power electric devices open the path to implementing a different kind of control on grid-connected PV systems, which can be divided further into other parts depending on the topology of the system. The first stage is to control the PV-array to extract maximum power depending on the DC-DC converter-booster stage. Alternatively, the inverter itself can perform the same task. [8].

The first topology is a two-stage compound [2], as shown in Figure 1.7.

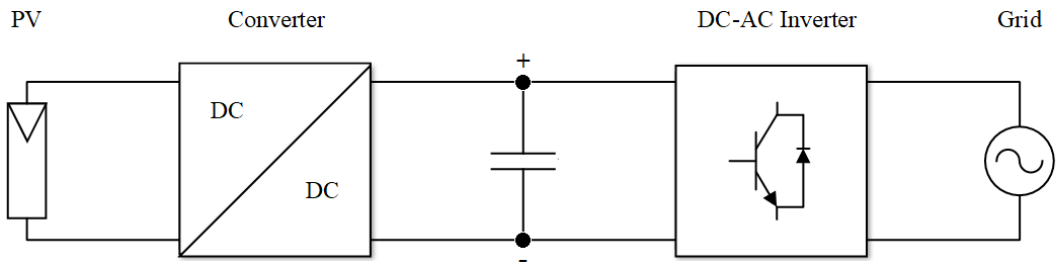

Figure 1.7. Two-stage converter to connect the PV-Array with the grid [2].

The second topology is as shown in Figure 1.8.

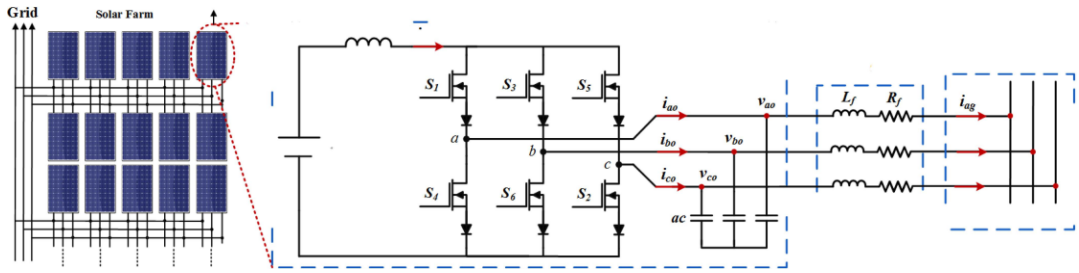

Figure 1.8. One-stage topology to connect the PV-Array with the grid [8].

The control methods used to control both of these stages can vary. Some are the traditional PI controls, but this method needs extra stages such as PWM, which has a bad dynamic response and study state error. However, this can be overcome using the proportional resonant controller (PR) [9][10]. In addition, the PID controller is a single-input single-output controller, which means it must use more than one controller to control each parameter of the system. It is not easy to contain system restrictions in this kind of controller. Another controller is the hysteresis controller, which is easy to

establish and implement with a simple algorithm. However, it has a switching frequency problem and needs an expensive wide filter to overcome this problem. The other controller is the neural controller, which is effective if any parameter of the system is unknown; but, it is rather complex [2].

This study focuses on another controller, namely the Model Predictive Controller (MPC), which has been known for quite a long time. The basic principles have been known since the 1960s and it received industry attention in the 1970s [2, 11] due to its interesting features, as follows:

- It is intuitive and easy to understand.
- It can work with more than one input and output.
- It is easy to include constraints.
- It does not need additional stages like PWM as in the PID controller case.
- It can work efficiently with linear and nonlinear systems.
- It has a fast dynamic response.
- It is easy to implement on a controlled plant.

The disadvantages of this type of controller include:

- A high number of calculations requirements to be implemented to obtain a result.
- Dependence on the system model, so its model must be accurate to gain sufficient control.

1.3. RESEARCH OBJECTIVE

In this research, the focus is on the following points:

- Develop a mathematical model describing an inverter connected to a local load via an LC-filter (stand-alone mode) and connected with the grid via an LCL filter to suppress switching harmonics (grid-connected mode).

- Using algorithm works in two modes: grid-connected mode and stand-alone mode.
- The usage of the FCS (finite control set) due to its simplicity combining with the one-step-ahead or residing horizon principle.
- Usage of ESS-energy storage systems (lithium batteries) controlled by a booster to deliver smooth DC voltage for the inverter (to overcome the intermittent problem of the PV-Array system).

PART 2

LITERATURE REVIEW

This chapter presents summaries of previous research conducted on the grid-connected inverter, its various types of control methods, and the applications used to control the inverter, which is a fundamental subject in renewable energy systems because it is the connection between renewable energy (RE) and the load or grid. Through this review, the motivation to use this kind of controller and the basic concept of the MPC will be illustrated. Moreover, this chapter present the idea of the MPC controller and its various types and how to implement them with electrical power converters.

The classical PID controller is well studied, easy to implement and can be tuned by MATLAB with more than one tuning technique. However, the disadvantage of this controller is that it works in a continuous domain (s domain) in a linear system only. Moreover, the converter is not a linear system (its switching system is followed by a filter). Therefore, we need first to linearize the converter with a different system, such as the PWM, and convert the reference signal in order to be suitable to work with the PID controller (Clarke Park transformation), which incidentally adds more complexity to the system. The PID controller is a SISO controller. Hence, we must use more than one PID controller. The PID is also sensitive to disturbance and considerable input variation. The major disadvantage of this kind of controller is that it has an inadequate dynamic response, and the system constraints such as maximum current, switching frequency and THD are difficult to incorporate.

2.1. PID CONTROL METHOD

In [12], the author used the PID controller with the VSI to inject pure energy into the grid by converting the nonlinear system (inverter) to a linear system via PWM, synchronizing the current with grid voltage using PLL (Phase Locker Loop) and using

Clarke-Park transformation. The control method is conducted by combining two controllers to form the cascade controller, which consists of an inner controller (to control the current or power quality (such as low THD and the unity power factor) and an outer controller to control the power (as shown in Figure 2.1).

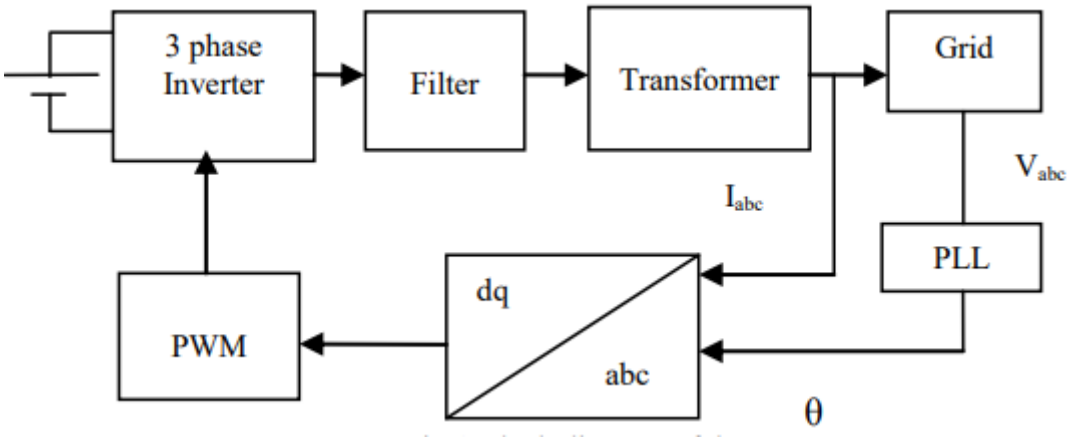

Figure 2.1. Block diagram of the inverter controller by PI controller [12].

The transformer here is a delta-star transformer, and it has three benefits, the first of which is to isolate the inverter from the grid and prevent injecting any DC into the grid, while the third harmonic circulates in delta and does not enter to the grid.

In [13], the researcher used the previous PID controller with PLL for synchronous purposes. The study presents a method of reducing the system's complicity by not transferring the three-phase system into a two-phase system (Clarke-Park transformation). Instead, he used three PI controllers on each phase (as shown in Figure 2.2) and also introduced a method to reduce the switching losses by applying the high frequency of the PWM on one of the switching drives while the others are in ON or OFF states. This would reduce the switching losses by approximately 33% by clamping one of the drives, as shown in Figure 2.3.

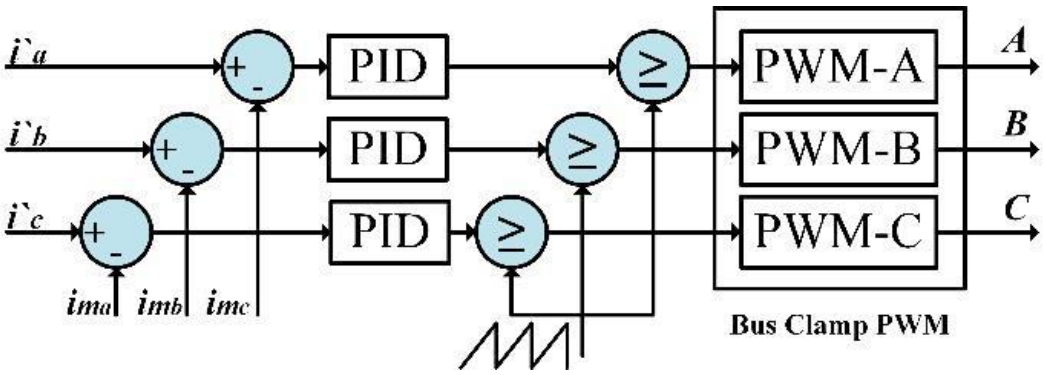

Figure 2.2. Employing three PID controllers instead of the d-q transformation [13].

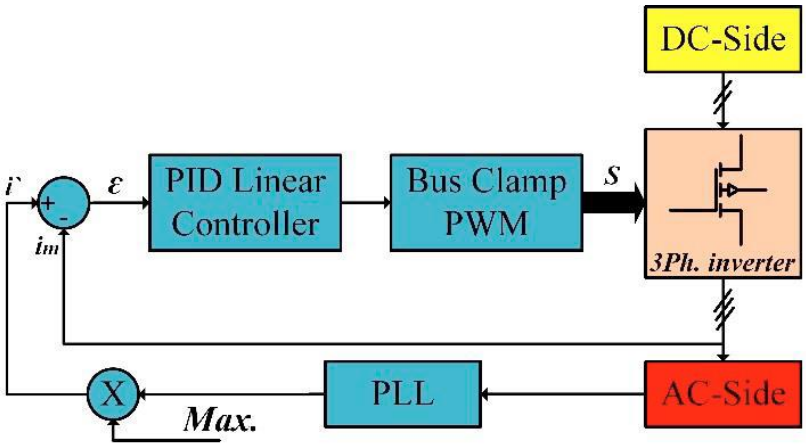

(a)

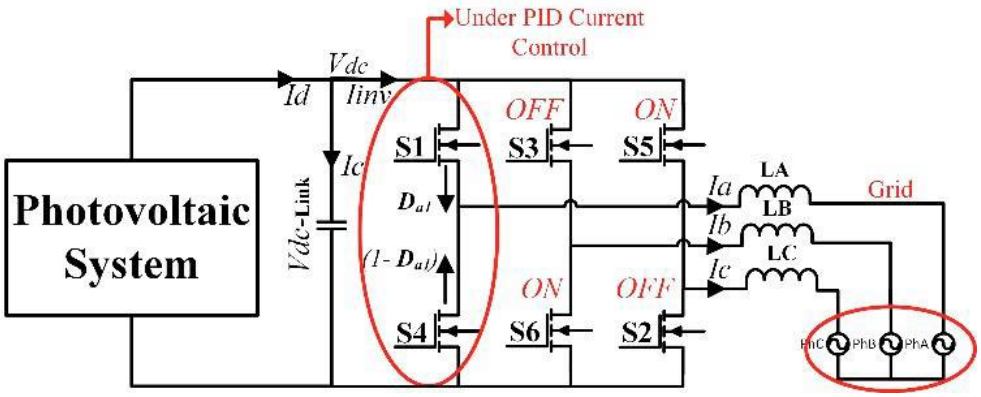

(b)

Figure 2.3. (a) and (b). The 120° bus clamping method reduces switching losses [13].

In the study by [14], the output of the booster is connected to batteries and then to the inverter to provide constant DC voltage without oscillation by controlling the booster voltage output via the PID controller by comparing the output voltage with the reference voltage, as in Figure 2.4.

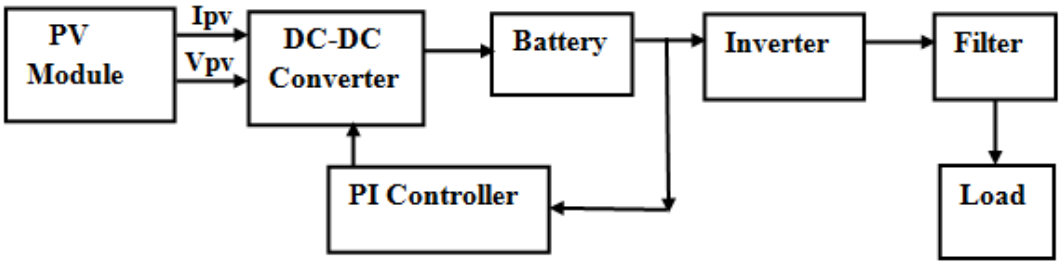

Figure 2.4. Proposed method to stabilize DC input voltage [14].

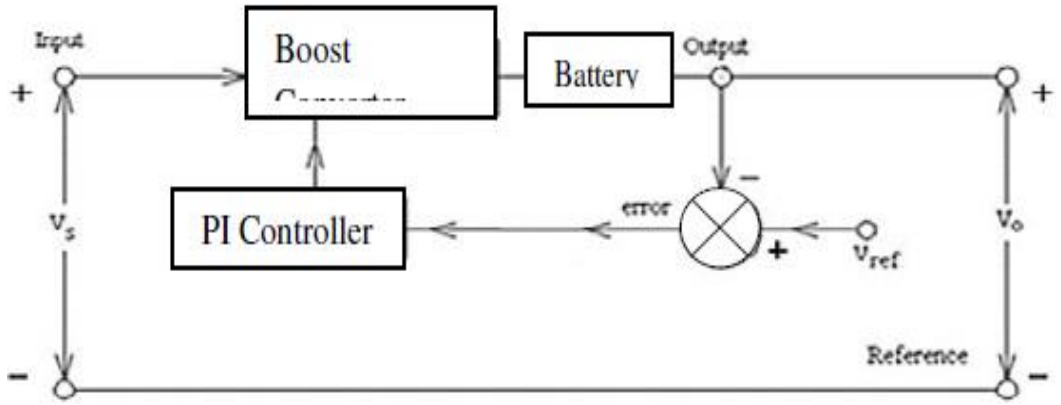

Figure 2.5. PI controller diagram [14].

The methods that are used to tune the PID controller include Particle Swarm Optimization (PSO) and Zeigler-Nichols.

In the study of [15], the PID control is combined with fuzzy logic to overcome the disadvantage of the PID controller, including the sensitivity to change in the tuning parameters, thereby improving the dynamic response (it becomes faster) and reducing the oscillation around the steady state.

The fuzzy controller here is used to determine the PI controller parameter by using the max-min method to calculate the PI parameter depending on the output of the converter as feedback (Figure 2.6) in which the input to fuzzy logic is $e(t)$ and $de(t)/dt$. The output is *Kp*, *Ki* and *Kd*.

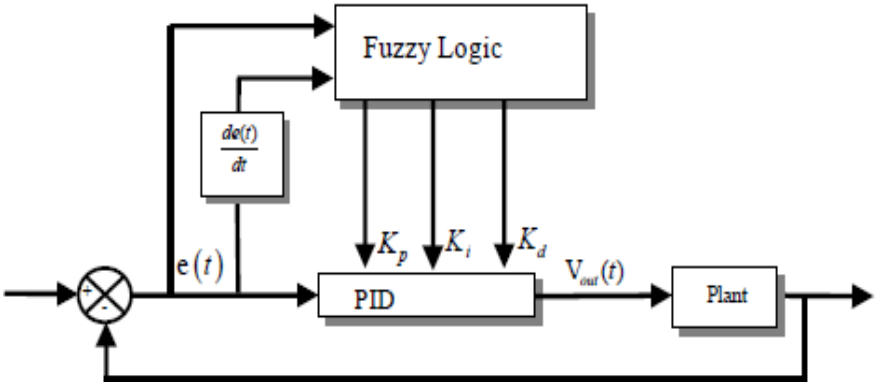

Figure 2.6. Combining fuzzy logic with PID controller [15].

In an approach by [16], more than one inverter connected to the grid is considered, (Figure 2.7).

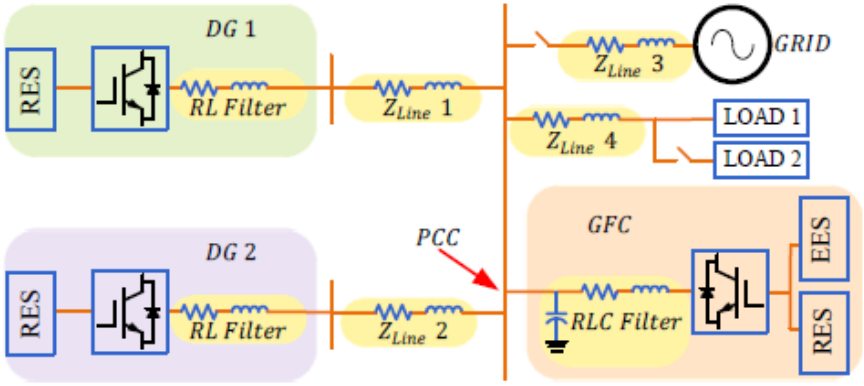

Figure 2.7. Renewable energy sources parallel connection.

Depending on the classical method (droop method) to synchronize more than one generator connected in parallel to feed the load, and explaining how the inverters will share the load depends on the relation between power-frequency and reactive power-voltage. in addition, the ESS used in this system ensures stability in case of isolated operation (when a fault occurs on the main grid) and the micro grid has to work in islanded operation mode to supply the load with power (in case of cut off from the grid) in stand-alone mode.

In addition, the storage energy system will store surplus power when the generated power exceeds what consumed by the load and vice versa, also to overcome load fluctuation as shown in Figure 2.8.

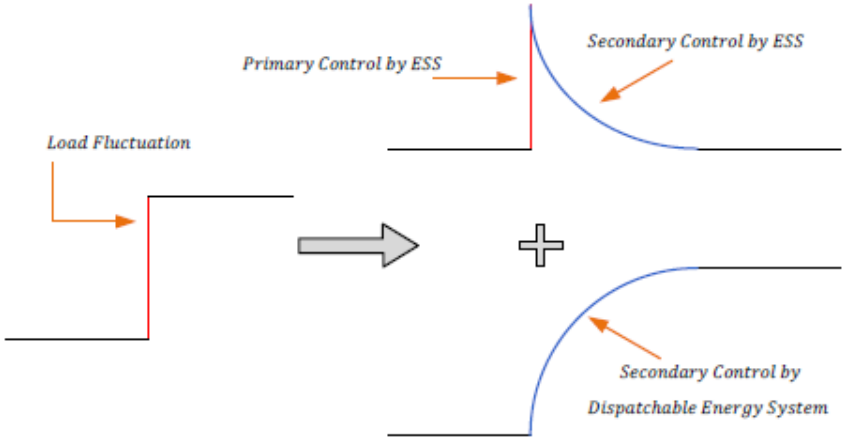

Figure 2.8. System responds in cases of load fluctuation (islanded mode) [16].

First, the three-phase grid voltage and current converter to the d-q system with PLL deduce the reference angle and magnitude of the voltage reference from the d-q conversion. The calculated power is used to calculate the inner frequency using the frequency-power equation, which is used to calculate the voltage command of the inverter.

Depending on cascade loops, that is, the outer loop for the voltage and the inner loop for the current, the Kp and Ki control parameters are calculated for the outer (voltage) and inner (current) control loop and used in both the q and d part, as shown in Figure 2.9.

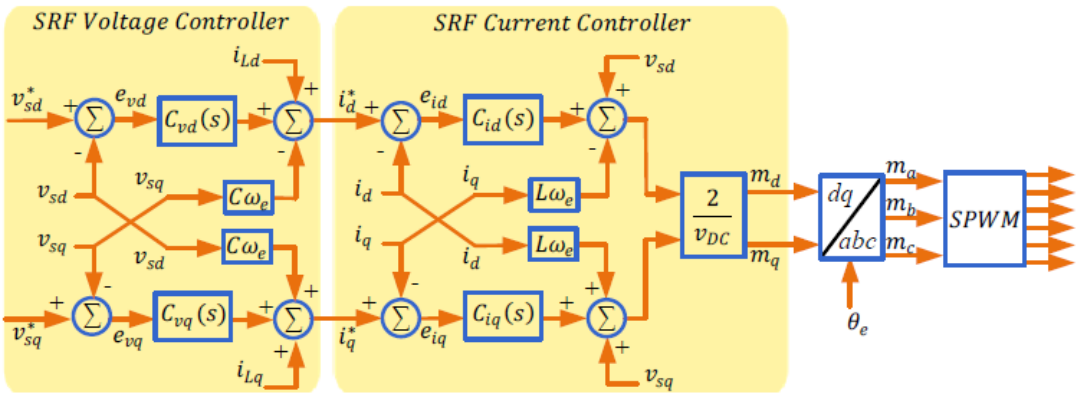

Figure 2.9. Block diagram for voltage and current control system [16].

2.2. THE MODEL PREDICTIVE CONTROL (MPC) METHOD

The MPC, or Model Predictive Controller, is the most attractive controller due to its advantages, including the following:

- It is intuitive and easy to understand.
- MPC can be applied to a variety of systems (flexible method).
- Constraints (limitations) and nonlinearity are easy to conclude and there is no need to add another system to linearize a nonlinear plant such as PWM, which makes the system easier to build.
- It is a multivariable controller, so there is no need to build a complex cascade controller.
- Control results are easy to implement due to their simplicity.
- It has a fast and good dynamic response because it can deal very well with non-linearity in the system.
- It combines the MPC controller with other control systems to optimize results, as in the Lyapunov stability theory.

The following are disadvantages of the MPC method:

- There are a high number of calculations.
- Its performance depends on the quality of the system model. The mathematical model represents the inverter, the connection filter or inductor, and the load or the grid.
- The variety of the output frequency makes it more difficult to design a suitable filter [17].

There is more than one type of MPC method. However, the main idea is the same, which is to predict the future behavior of the system and calculate the most suitable order according to the optimization function (cost function) so that the MPC does not depend on the error. In fact, it prevents it from occurring in the first place [17].

2.3. TYPES OF POWER INVERTERS

The inverter can be classified into more than one type depending on its size (central converter, single phase (usually a few kilowatts) or three phase converter (usually 5 kW to 100 kW) or micro-inverter, about 300 watts, and can be classified according to converting stages between the PV-array and the grid or the load.

- Two Stages Inverter

1- The booster stage, the main job of which is to optimize the power produced from the PV-array and control the voltage to deliver it to the inverter.

2- The inverter stage connects the booster, PV-array and the grid by converting DC to AC voltage by synchronizing voltage, frequency and angle.

- The single stage inverter does both jobs mentioned above in a single stage without needing to a booster stage. Sometimes the second stage is preferred, especially in low power inverters such as micro-inverters (300 W or less) due to their simplicity, low cost, mass production, high efficiency and small size.[8, 18] The MPC method is flexible and can be combined with other control methods such as the Lyapunov stability method. The sphere decoding method [17] is easy, feasible and easy to implement.

In [19], only one stage converter is used with the control combining two methods, namely the perturb and observe (P&O) and the MPC method. The P&O algorithm provides the reference current to the MPC controller, which provides the switching signal for the inverter drives. The result of this work is a high dynamic response due to the fast response of the MPC method with high efficiency, which is 98% for MPPT and 92% for the inverter, which means 90% of total system efficiency. Figure 2.10 shows the general configuration of the system.

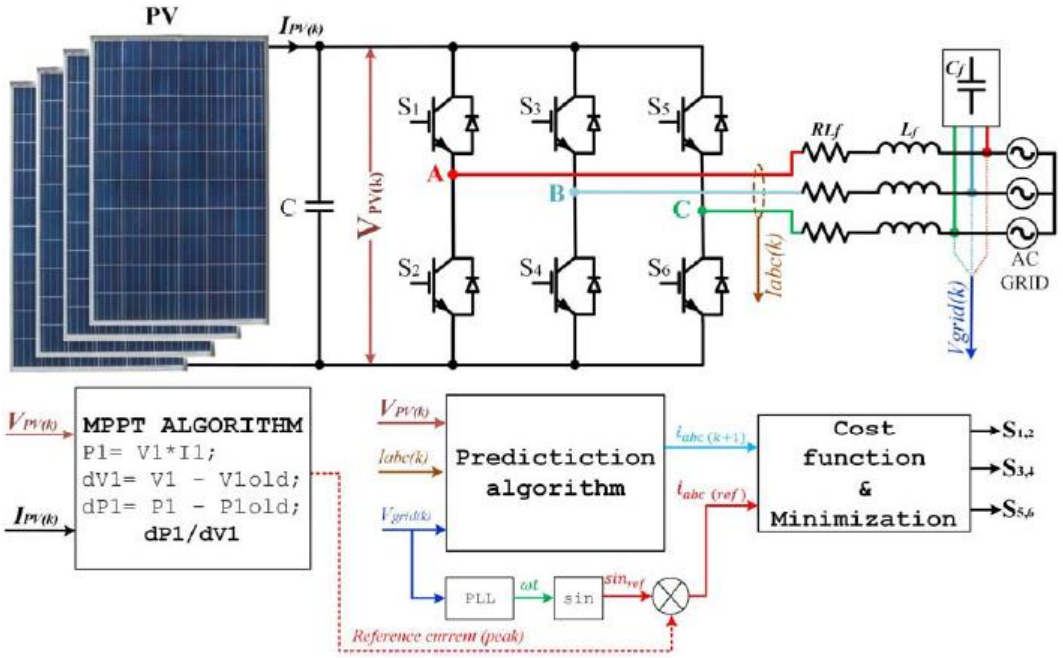

Figure 2.10. Single stage converter of a PV-array system using P&O and MPC methods [19].

In [8], a one stage converter, as in the previous work, is proposed. The researchers used a Model Integrated Converter (MIC) or a Micro Converter. In it, the converter is built into the solar array itself to have advantages such as low cost, mass production, improved system stability and elimination of single point failure. This work expanded the use of a single-phase converter into a three-phase inverter by using the Current Source Converter (CSC), which uses inductance to boost the DC voltage to grid voltage (Figure 2.11).

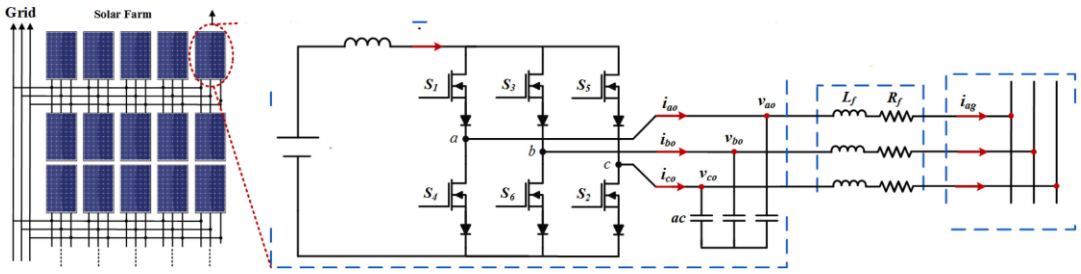

Figure 2.11. Three-phase current source microinverter [8].

In only a single stage and at the same time combined with low voltage riding through (LVRT) to provide the necessary reactive power during the fault time to ensure grid stability, the control method is a finite control set model predictive controller

(FCS-MPC) working on the d-q transformer (Park transformer) with PLL to deduce theta. The switch of the combination is nine switching combinations, namely three for the charge to boost the voltage booster work, and six is for discharging or converting DC to AC (inverter working), as shown in Figure 2.12.

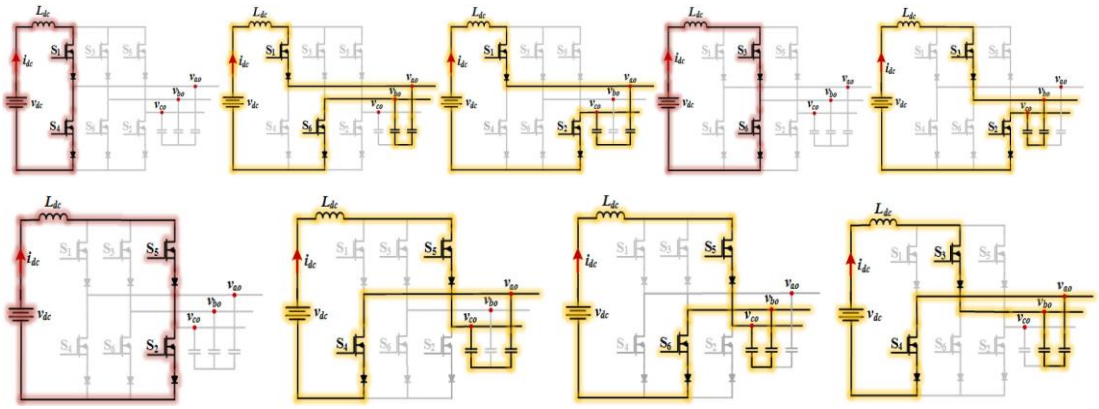

Figure 2.12. Charging and discharging operation states of CSC – based MIC [8].

This method reduces losses due to using a one-stage, not a two-stage converter, and fewer switching drives, specifically six drives instead of seven (in the two-stage converter), which reduces the cost.

A two-level, three-phase inverter is used to connect the PV-array with the grid [18]. it uses the Perturb and Observe algorithm to obtain the MPP from the PV-array. However, when combined with the booster and the inverter, it is controlled by the MPC using the Park transform to control the inverter with a finite number of switching theories (FCS-MPC) and the inverter containing the transformer which is used to isolate the inverter from the grid in fault cases and to have matching between the inverter voltage and grid voltage (450 V is the inverter voltage and the grid voltage is 600 V), as shown in Figure 2.13.

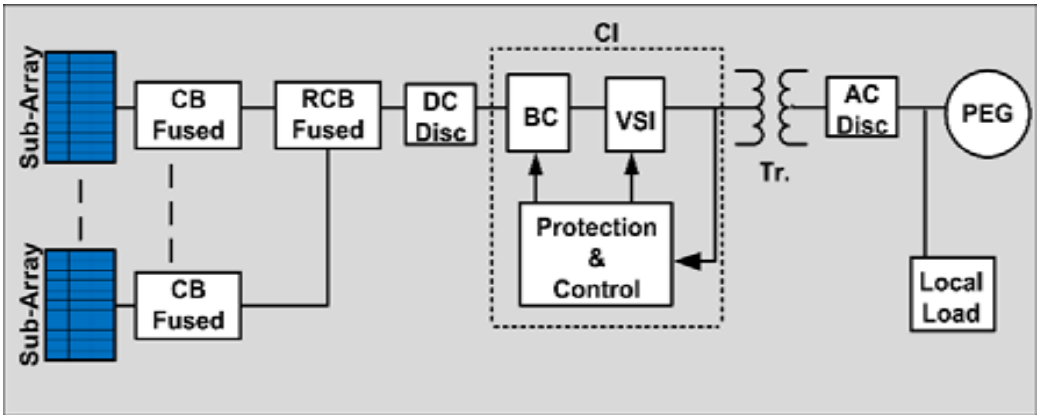

Figure 2.13. Structure of the three-phase inverter combined with booster [18].

The classical MPPT method does not consider the impact of changes in environmental conditions (such as irradiation, temperature or wind speed) on the system tracking speed and accuracy. This therefore presents a method to combine the MPC with MPPT to improve the speed and accuracy of tracking the MPP by considering the environment incident on the PV-array to optimize the power generated from the PV-array (Figure 2.15) [20]. The finite control set model predictive current control (FCS-MPCC) method in comparison to classical feedforward with a PI controller shows the advantages of using the MPC method. Advantages include quick response, high accuracy, flexibility, and good dynamic response.

The construction of the system is shown in Figure 2.14.

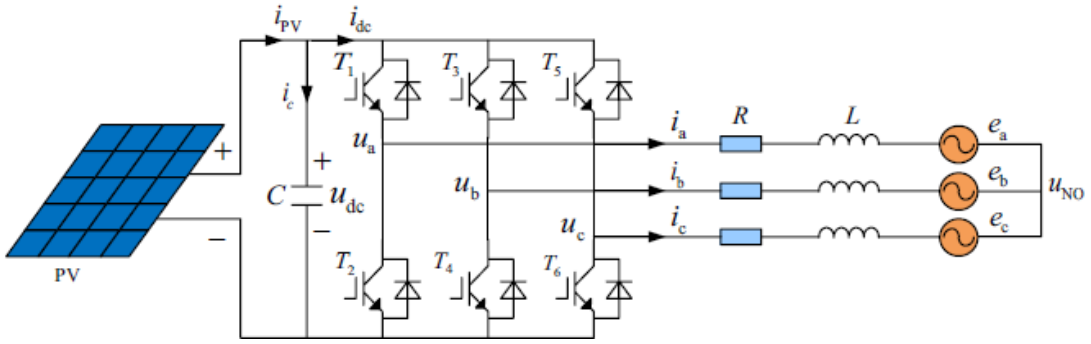

Figure 2.14. System construction of the PV-Array grid connected following the MPC control method [20].

The system algorithm depends on the d-q transform. The MPPT has become the critical method to optimize the power withdrawal from the PV-Array. However, the

temperature harms the power generated by the PV-Array, so here the MPC method is used to predict the effluence of different irradiation incidences on the PV-Array temperature and to generate power to control the active filter to reduce the PV-Array temperature and generate maximum power simultaneously by modeling the PV-Array, as shown in Figure 2.15.

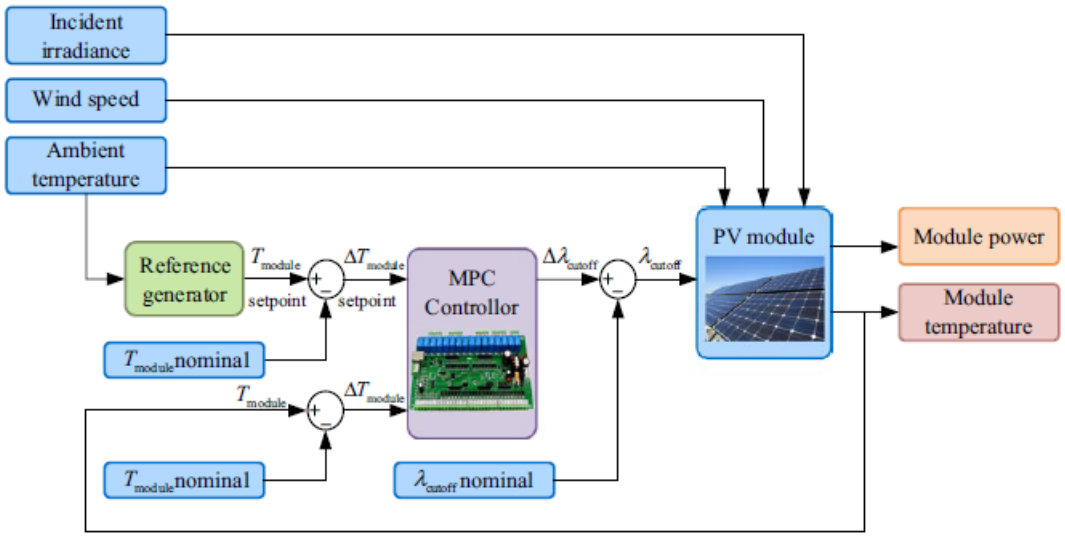

Figure 2.15. Modeling of the PV-Array following the MPC method [20].

Figure 2.16 shows the feedforward method to control the inverter. The feedforward method is used to compare it with the result from the MPC method.

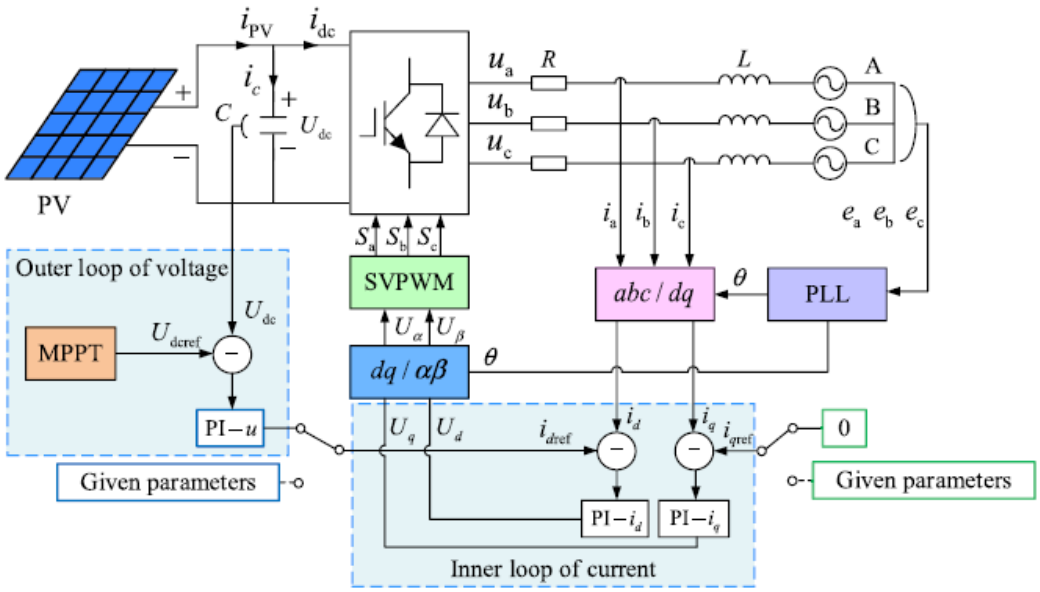

Figure 2.16. Feedforward decoupling control method based on the PI controller [20].

As shown in Figure 2.16, the control method contains two loops: the outer loop, which is the PV-Array DC voltage loop used to deduce the reference current, (the inner loop) to maintain power quality such as the unity power factor and low THD.

The MPC controller depends on an algorithm to reduce the output current error depending on the cost function via an alpha-beta transformer with one PI controller to generate the reference current with PLL finding theta (the PI and PLL used in both strategy feedforward and MPC), as shown in Figure 2.17.

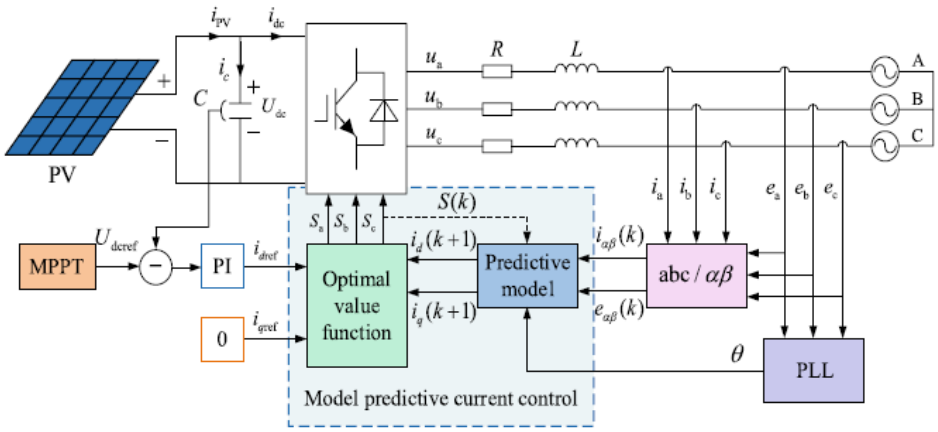

Figure 2.17. FCS-MPCC structure of the PV-array grid [20].

The simulation result shows the advantages of the MPC, which include its rapid speed response for changes in operation conditions during grid faults, stable generated power, and for the PV-Array, increases in tracking sensitivity of the MPP and better performance.

For the PV-Array, [21] uses a combined incremental conductance, model predictive control algorithm (IC-MPC) for very high precision and fast response in tracking the maximum power point. The second part compares the classical VOC (Voltage-Oriented Control) depending on the classical PI controller, SMC (Sliding Model Controller), and MPC (Model Predictive Controller), as shown in Figure 2.18.

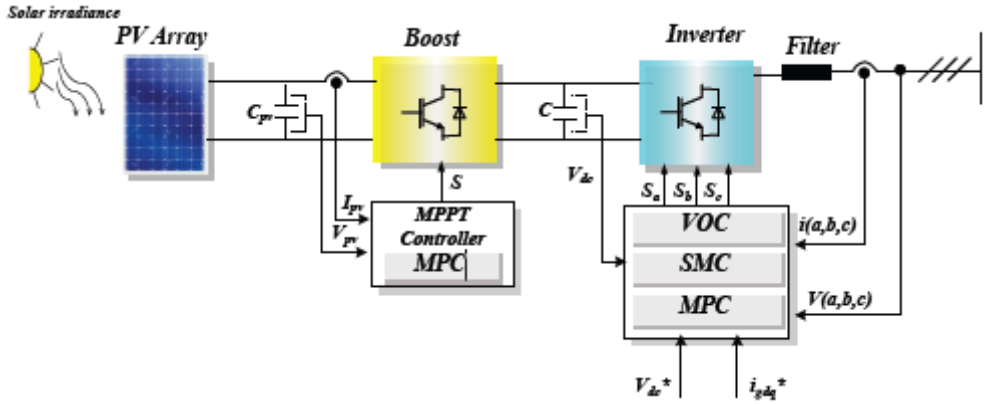

Figure 2.18. Construction of the PV-array grid-connected inverter with suggested control methods [21].

The sliding control mode (SMD) is suitable for overcoming the change in circuit parameter. However, its main issue is high THD, at approximately 7.8% [21] with overshot better than the VOC method. However, the harmonic is better here at approximately 5.6%. For the MPC method, however, it is 3.7% with a better overshot. The authors of [22] propose a solution to overcome the disturbance, the uncertainty in converter components, such as the inductance or the capacitance due to error or aging. These two factors degrade system performance and may even drive it to instability. Different kinds of control methods are discussed here. The PI & PR controller usually use cascade control loops. The inner loop (the current control loop) is used to overcome any disturbance and enhance system stability, while the outer loop (the voltage control loop) produces the reference to the inner loop and achieves zero steady-state error. However, these methods are linear, so another system needs to linearize the converter (the PWM). Due to this, it results in less-than-ideal dynamic responses and necessitates the use of extra hardware components to overcome harmonic responses during dynamic transit. Moreover, these are usually designed in the continuous time domain, so they are difficult to implement with microprocessors, which are usually used in modern control systems. On the other hand, the MPC controller is excellent, coinciding with a discrete control method and ease of digital implementation. Among the advantages, the constraints are easy to implement and are intuitive. However, the disadvantage is that the MPC controller depends on the system model, so it is sensitive to system component mismatch and control system delays, which may degrade system performance or cause instability. Moreover, it needs current sensors to provide a good disturbance rejection, which increases the system size, increases cost and measurement

losses. The SMC (Slide Model Controller) is good at overcoming parameter uncertainty and unknown distribution problems, but chattering problems with tracking variables are the significant problems of this kind of controller. This paper proposes an augmented state-space model and the adaptive observer in a three-phase LC-filter to overcome previous problems. The adaptive MPC controller combine all the uncertainty of the system and reduce the need for more sensors, thereby reducing system cost and elevating system efficiency and reliability.

Figure 2.19 below compares conventional and adaptive MPC controllers.

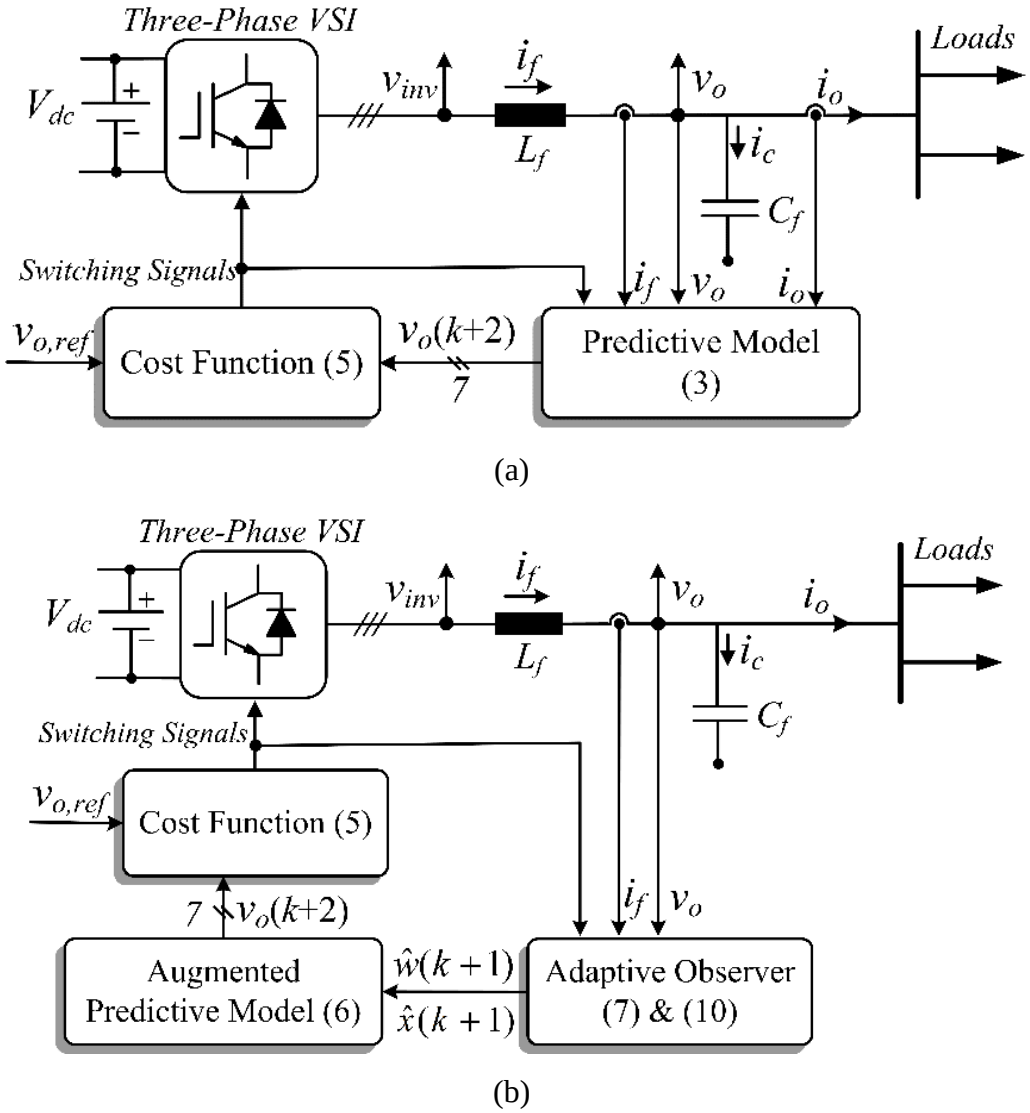

Figure 2.19. (a) Conventional MPC controller; (b) Proposed adaptive controller [22].

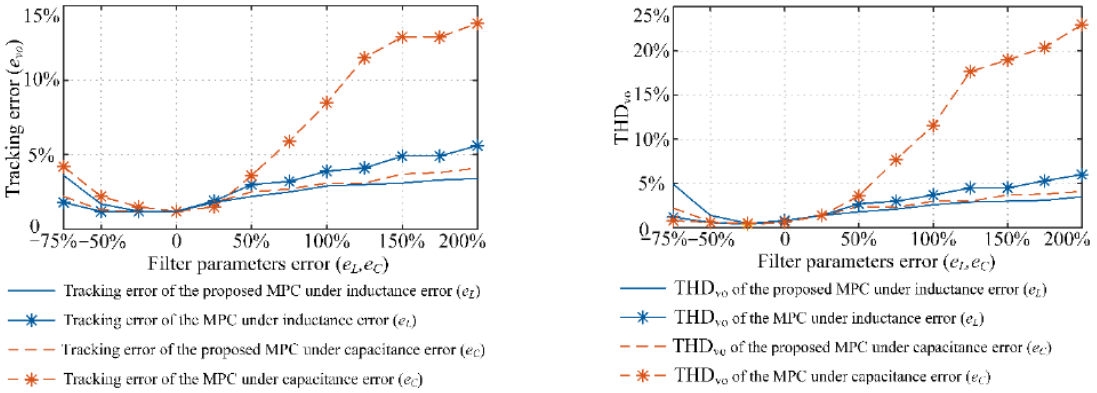

Figure 2.20. Comparison of conventional and adaptive MPC controllers [22].

As shown Figure 2.20, the tracking error is better in the proposed MPC method than in the conventional method by about twice the traditional value, which proves the efficiency of this adaptive method. However, the cost of increasing the calculation burden is approximately twelve more operations; however, it enhances the dynamic response and overcomes any uncertainty in component parameters and disturbance.

[23] proposes the Continuous Control Set Model Predictive Controller (CCS-MPC) combined with the LCL filter and compares it with FCS-MPC. Due to the increasing demand for clean energy to reduce greenhouse gas emissions and elevations in regulation on grid-connected inverters, LCL filters are increased for better filtering of harmonics. However, one disadvantage of this is resonance, for which we can use the passive or active damping method in order to overcome this problem. Moreover, the passive resistor, which is not accepted because of power losses or active damping, which depends on the control damping algorithm. The MPC method is promising because it has a fast dynamic response, it is easy to understand and implement, and it is easy to contain constraints in the MPC cost function. The primary disadvantage, however, is the switching frequency, which is not constant. This paper suggests a CCS-MPC to control the switching frequency and simultaneously reduce harmonics compared with the conventional FCS-MPC method. However, this comes with the use of SVM, which is achieved by using the Kalman filter as an estimator due to its advantage in a noisy environment. Moreover, it reduces the switching noise at the same time (as shown in Figure 2.21).

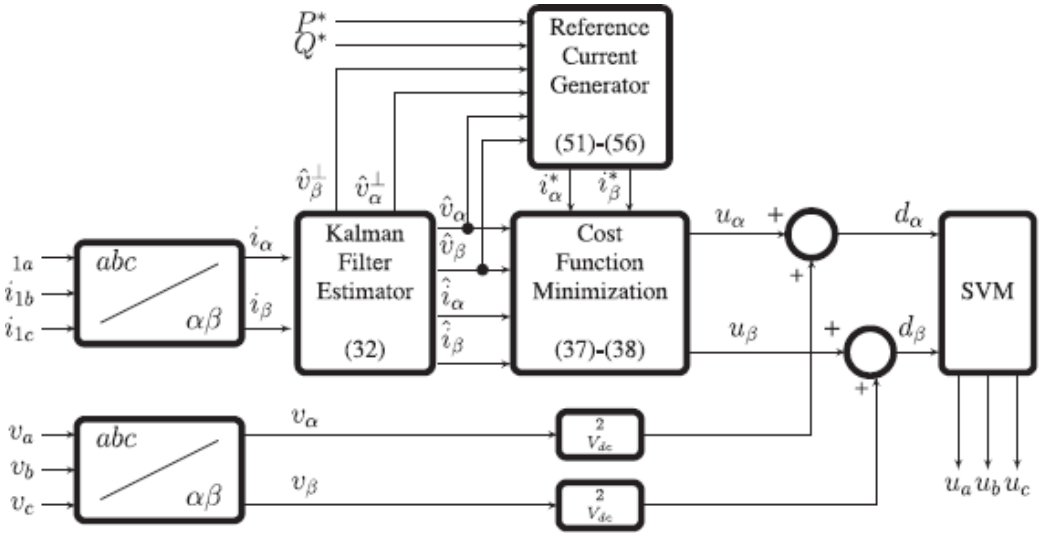

Figure 2.21. Construction of a three phase inverter with an embedded Kalman filter [23].

As we can see, the three-phase voltage and current are transferred to α-β transformation and used by the Kalman filter to produce the reference current and voltage. To overcome the harmonic issue, the feedforward method is used to mitigate this problem (see Figure 2.22).

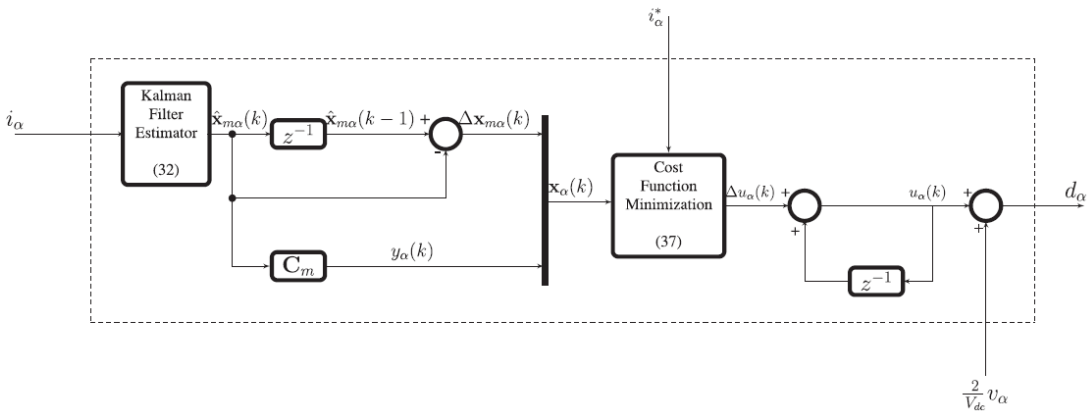

Figure 2.22. Feedforward to reduce current harmonic embedding [23].

The suggested method reduces the calculating burden, fixes switch frequency reducing switching noise, with a fast dynamic response and wide bandwidth without needing to change algorithm parameters. Reducing switching frequency reduces the LCL filer component. In addition, this method does not require any PI or PR controller.

This paper [24] uses the MPC method to design a robust estimator to control a three-phase grid-connected inverter with an LCL filter to cut off disturbances, which may divide into three parts the uncertainty in filter parameters values (the inductance, capacitance, and resistance of the LCL filter). The second part is the uncertainty in the system model and grid voltage disturbance. The LCL filter has excellent harmonic attenuation performance; however, it is a three-order filter which leads to the resonance problem and grid voltage disturbance that may cause more instability. The PI controller is easy and well-studied but has poor dynamic and harmonic rejection, especially for high-frequency harmonics. The PR controller is suitable for the rejection of harmonics. However, it must be tuned to every frequency that needs attenuation, leading to more complicity and steady-state errors. The adaptive controller is very good at tracking grid voltage, and the H-infinity controller is good at overcoming the control system's uncertainty. The MPC is very good at forecasting the system's future behavior as it can deal with the nonlinear system, so there is no need to linearize the design. Additionally, it is very good at rejecting the disturbance hover. It is sensitive to time delays, and its performance depends on system model accuracy. This paper presents an MPC controller with a robust disturbance observer design following the LMI method. The PLL tracks the grid voltage angle used to convert the three-phase system to d-q for the MPC controller's disturbance rejection estimator to calculate the PWM's duty cycle, as shown in Figure 2.23 below.

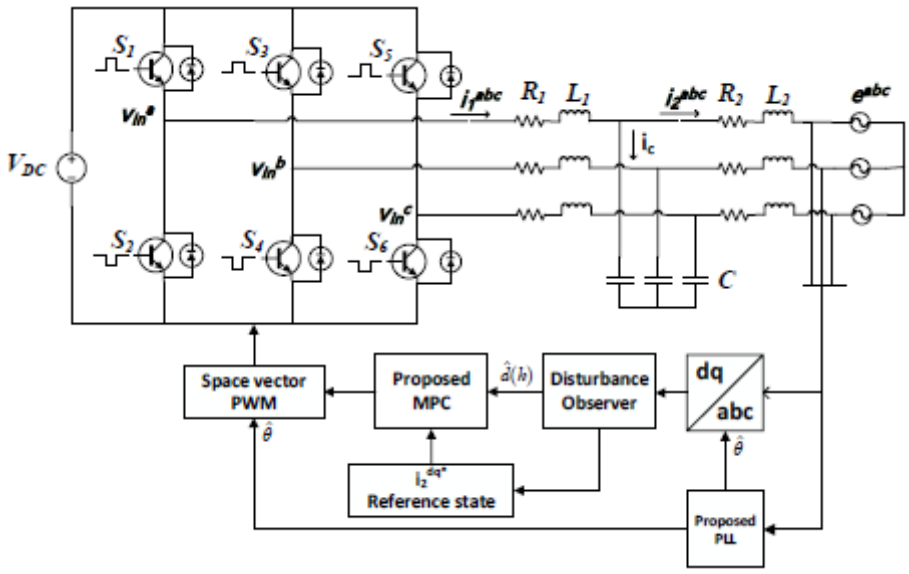

Figure 2.23. Proposed system for disturbance observer rejecter with MPC controller being embedded [24].

The result of this work is compared with PI controllers. PI controllers suffer from isolation during the transient time and this leads to reductions in power quality. The usage of the MPC controller with robust disturbance observer overcomes the uncertainty in the system model and grid disturbance with excellent tracking performance.

Renewable energy (RE) needs to connect with the grid due to its intermittent nature via an electric device (the inverter) [25]. However, the quality of power injected into the grid needs to be considered and regulated, and this power quality depends on control strategy and modulation. Classical control methods, such as PI and PR, rely on the control coefficient and have bad dynamic responses. Enhancing the dynamic response leads to a higher overshot, which may cause damage to inverter drives. While the hysteresis control has a good dynamic response, the switching frequency is difficult to control. This paper presents an MPC method with a cost function to reduce the switching losses using the cost function and compares the suggested method with the hysteresis method. The major disadvantage of the hysteresis method is the switching frequency, which is difficult to control, especially with a low level of current (this method is considered unpractical for low load applications). One method to overcome this problem is to use the adaptive hysteresis method with three HCs on each phase, as shown in Figure 2.24 below, which makes switching states difficult to control.

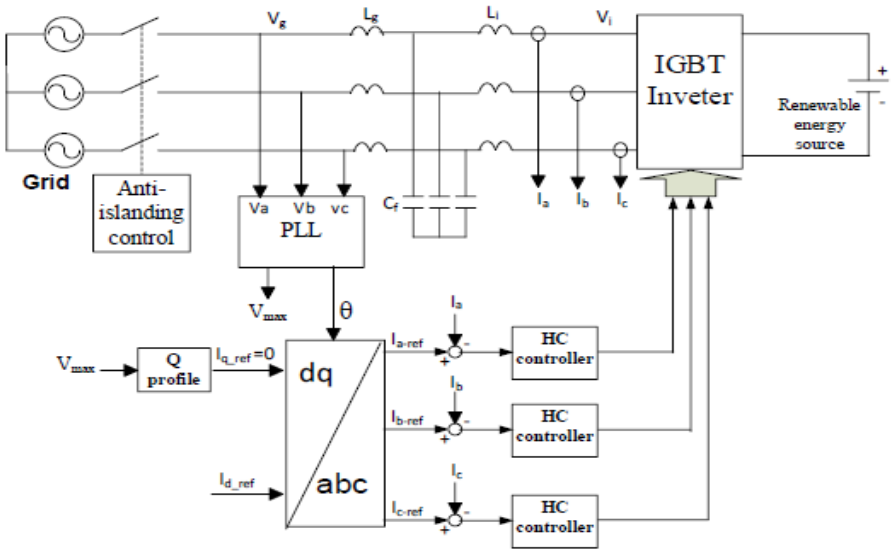

Figure 2.24. Three-phase inverter with hysteresis control on each phase topology embedded [25].

The development of digital platforms such as the DSP makes it possible to overcome the MPC controller's calculation burden, thereby leading to an increase in popularity, fast dynamic response, and rejection to control loops (cascade loops). The algorithm used in this work is shown in Figure 2.25 below, and it is used to reduce switching losses by identifying a parameter in the cost function (λ), which is used to reduce switching frequency.

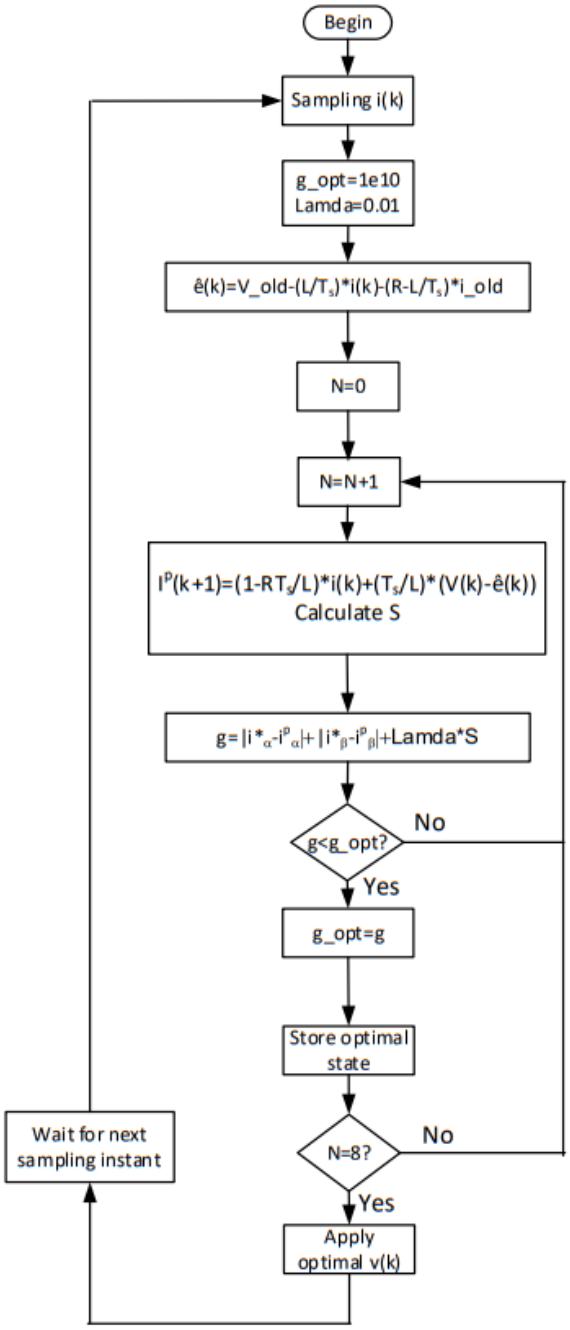

Figure 2.25. MPC algorithm with switching factor combined with cost function embedded [25].

Here, λ is equal to 0.01 multiplied with the switching state is combined into the cost function, thereby reducing switching frequency and harmonic and switching losses.
[2] presents an overview of Model Predictive Control (MPC) type FCS-MPC (finite control set model predictive control) and compares it with other types of controller mentioning its advantages and disadvantages such as the linear controller (PI), which needs to linearize the system (the inverter) by adding a modulating stage (pulse width modulation (PWM)) in addition to other types of controller such as the sliding controller model, hysteresis controller, and neural controllers such as the fuzzy controller. These types of controller have advantages such as robustness and overcome unknown model system parameters such as inductance, capacitance and resistance. However, they are complex, infected by changes in operating conditions and loads, and are infected by chattering frequency. The MPC controller is intuitively easy to understand and does not need a modulation stage such as the PI controller. However, the main disadvantage is that its performance depends on system model accuracy. Therefore, on occasion in order to overcome this problem, it needs an estimator or adaptive controller. The main disadvantage is the complex calculations required to predict the next step. This work presents a method to optimize the analysis of the FSC-MPC method using the sphere decoding optimization algorithm. This method reduces the calculation burden of the MPC controller by reducing possible switching states. The FSC-MPC works on the number of switching states and selects the optimized choices (i.e., those that produce minimum error) depending on the cost function.

The majority of the MPC algorithm depends on the one step forward control method to avoid the huge amount of calculations that the system needs to perform to achieve more than the one-step control horizon (the calculation will increase exponentially with an increase in the controlled horizon), as shown in Figure 2.26, which is for three-level inverters of the three-step forward controlled steps.

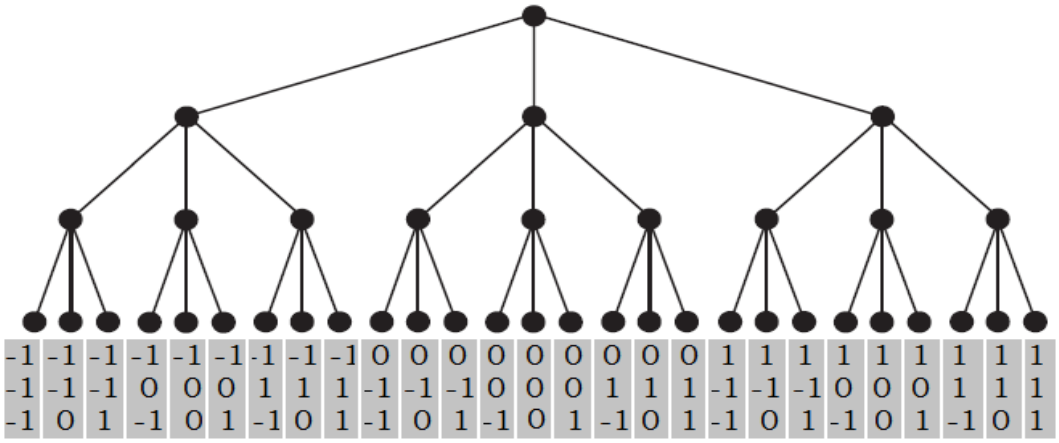

Figure 2.26. Possibility tree of the switching state of the three-level converter with three steps forward [2].

To overcome this considerable calculation, the work presents an optimization control algorithm (sphere decoding) that borrows from the communication field to prune useless branches in the early stages.

The LCL filter has very good harmonic attenuation performance, which makes it practical to use with a grid-connected inverter to meet modern control system regulations [26]. However, one disadvantage is the resonant frequency which may cause a degrading of the performance of the system or even cause instability, especially when connected with the grid with a large percentage of injected power. There are two primary resonant harmonics grid side inductance-capacitance resonances. The second is a converter side inductance-capacitor operating according to the following two laws:

$$\mathbf{w1} = \frac{\mathbf{1}}{\sqrt{C * L2}} \qquad \mathbf{w2} = \frac{\mathbf{1}}{\sqrt{C * \frac{L1 * L2}{L1 + L2}}}$$

where L1 = Converter Side Inductance, L2 = Grid Side Inductance, and C = Filter Capacitor, as shown in Figure 2.27.

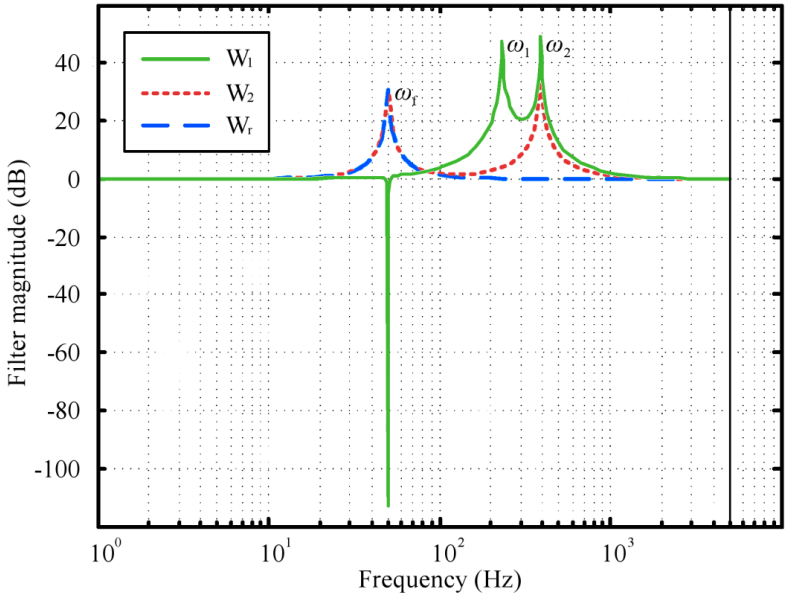

Figure 2.27. Main resonant component of the LCL filter [2].

To overcome this problem, there are two methods. The classical method is passive and adds resistance to the capacitor to dissipate the resonant frequency. However, this method is not favored because of efficiency problems due to dissipated energy and the addition of hardware in the form of a resistor.

The active method is therefore more favored by connecting a virtual resistor in parallel with a filter capacitor to dissipate the capacitor current (Figure 2.28).

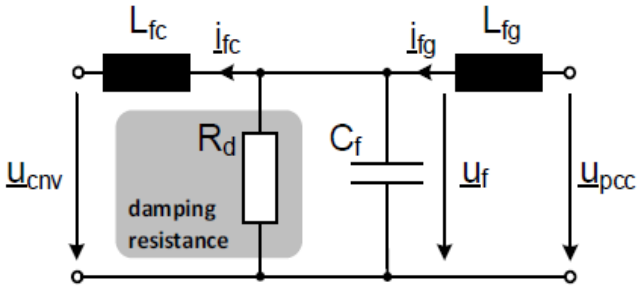

Figure 2.28. Active damping method to overcome the LCL filter resonant problem [26].

The active damping method is more favored. This work presents the MPC method with three feedback approaches to overcome the resonant frequency problem by embedding a low pass filter inside the cost function to filter the resonant frequency. The second approach is to add virtual resistance in parallel with the filter capacitor, which is carried

out by the injected current in phase with the grid voltage, and finally by controlling the voltage and current component on the converter side (two state space of the LCL filter states) via cost function, leading to control of the resonant frequency or its damping thereby achieving better dynamic response and reducing harmonic and switching losses by reducing the switching frequency to 1.6 kHz.

In the study by [27], a reduction was made to the LCL filter order to the first order system, considering it an inductance filter, and adding a disturbance equation to the control algorithm to represent the resonance distortion. The control design combines the MPC feedback algorithm with disturbance rejection, which resulted in good tracking performance and good damping performance.

The researcher(s) in [28] used predictive direct power control (PDPC) to deduce maximum power from a grid-connected PV-array system using Lyapunov theory to produce maximum power from the PV-array and inject it into the grid. The advantage of using the Lyapunov approach in reducing the calculation is to predict the future actuation value. This method proved to be significantly effective has a high-speed dynamic tracking response, with high robustness against system parameter variation, and simultaneously using a one-stage inverter, as shown in Figure 2.29.

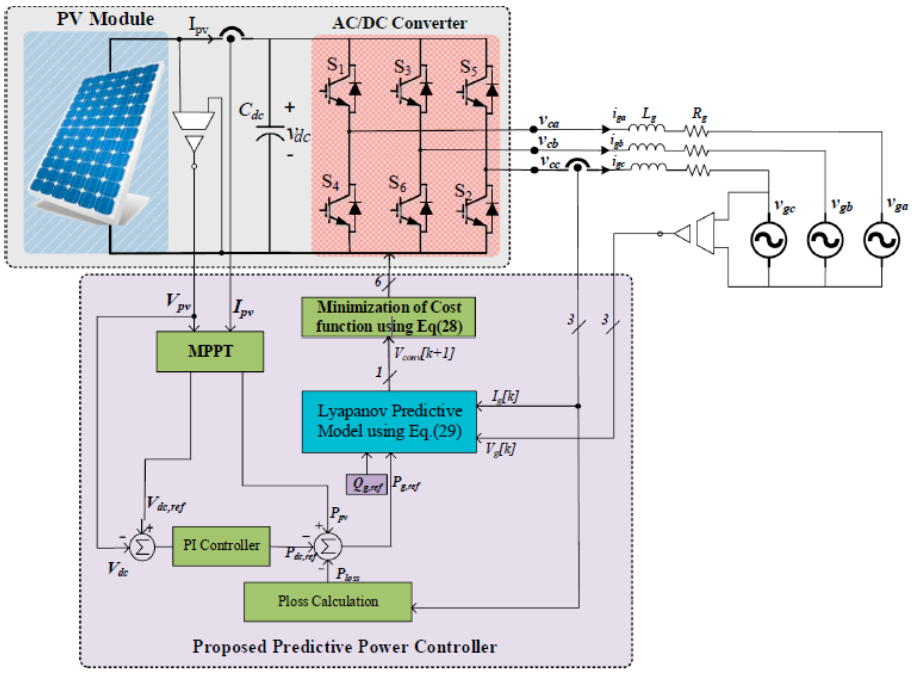

Figure 2.29. PDPC using MPC via Lyapunov theory [28].

The logical diagram of this algorithm is shown in Figure 2.30.

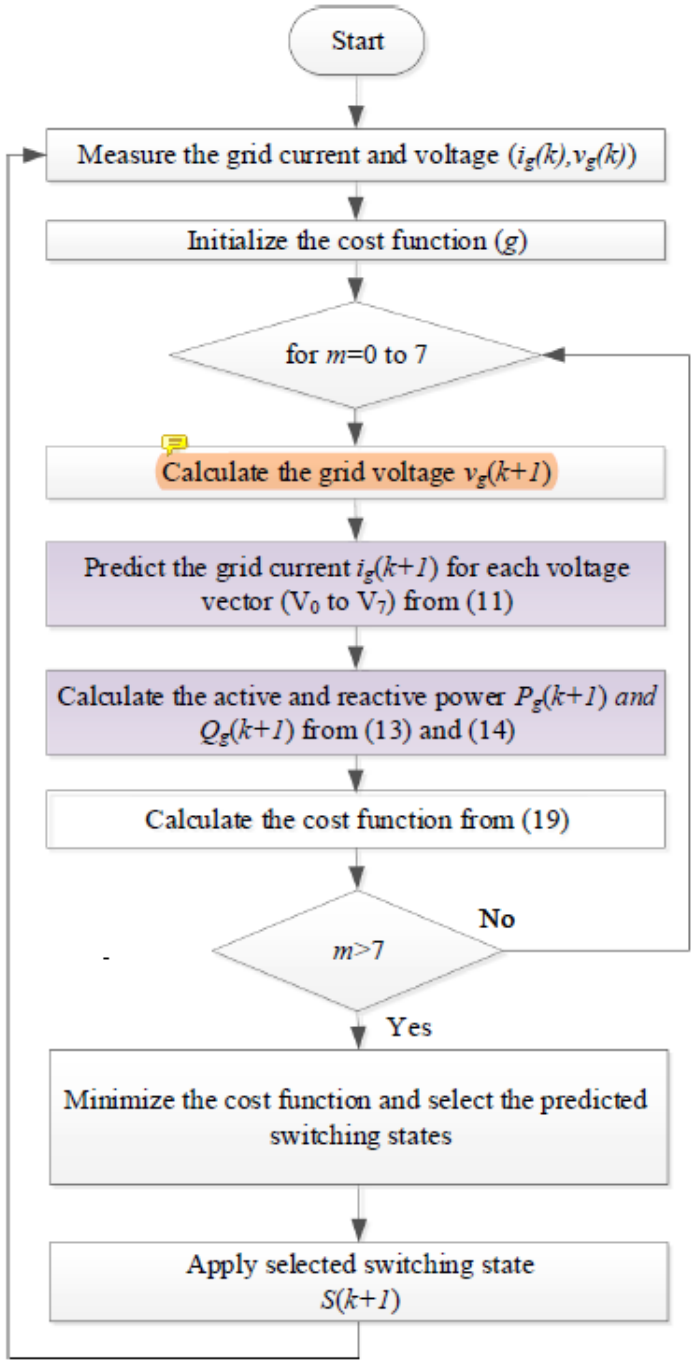

Figure 2.30. Logical diagram for the PDPC method [28].

In [29], work was performed by an MPC controller algorithm by applying directly to the inverter drives to overcome the delay time which occurs in control systems due to modulation stages as required in PI controllers.

The PID controller needs to linearize the system. Moreover, any poor modulation and analog-to-digital converter problem (delay problem) can be overcome by using the MPC controller due to there being no requirement for a modulation stage and it can be implemented directly to the system.

This work also works with an estimator for the capacitor voltage of the LCL filter to reduce the sensing devices. This elevates system reliability and reduces the amount of hardware needed to build the system.

Figure 2.31 illustrates the construction of this system.

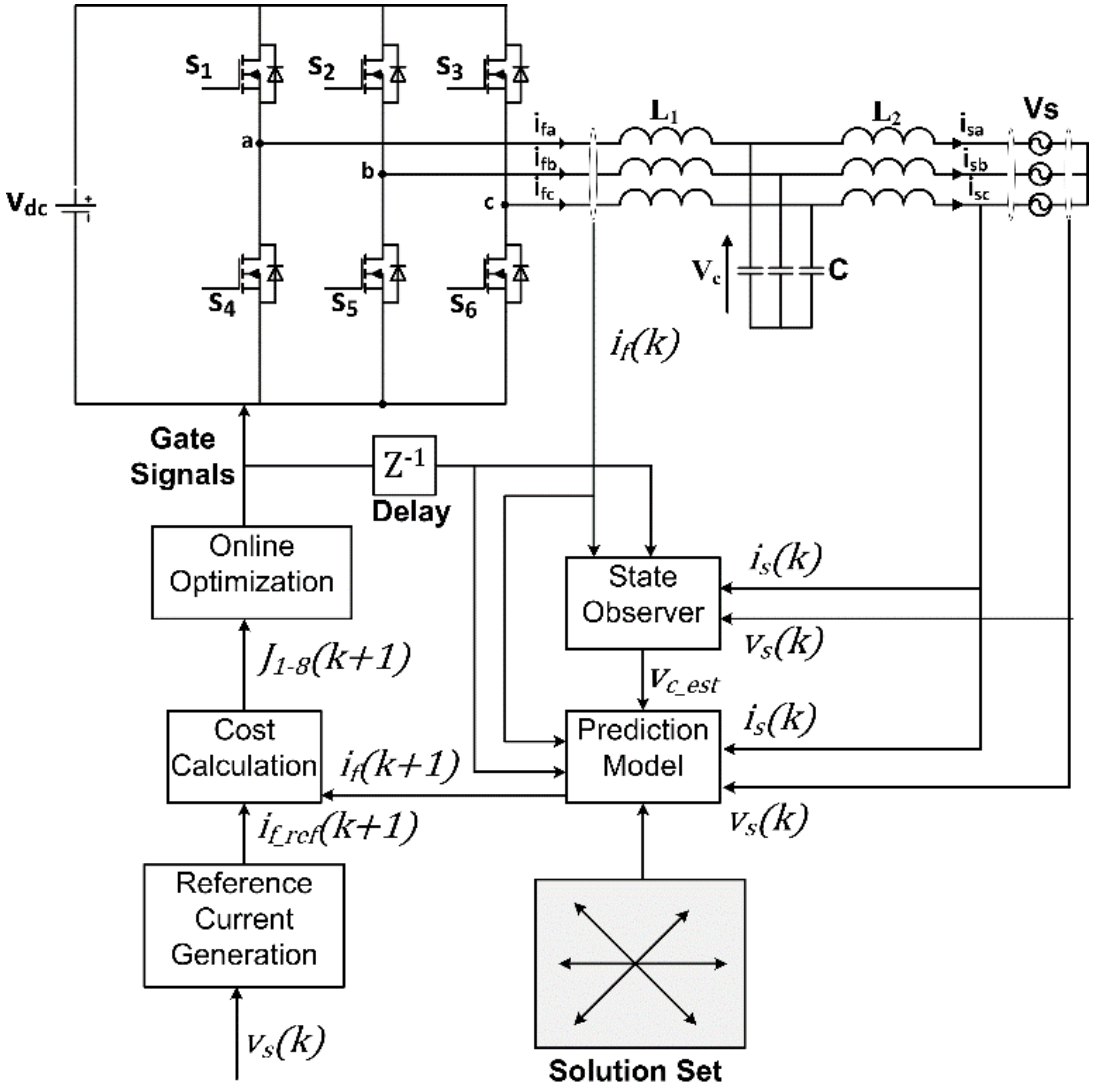

Figure 2.31. Construction of the MPC controller using a capacitor voltage estimator [29].

Figure 2.32 illustrates the reference circuit used to produce the reference current.

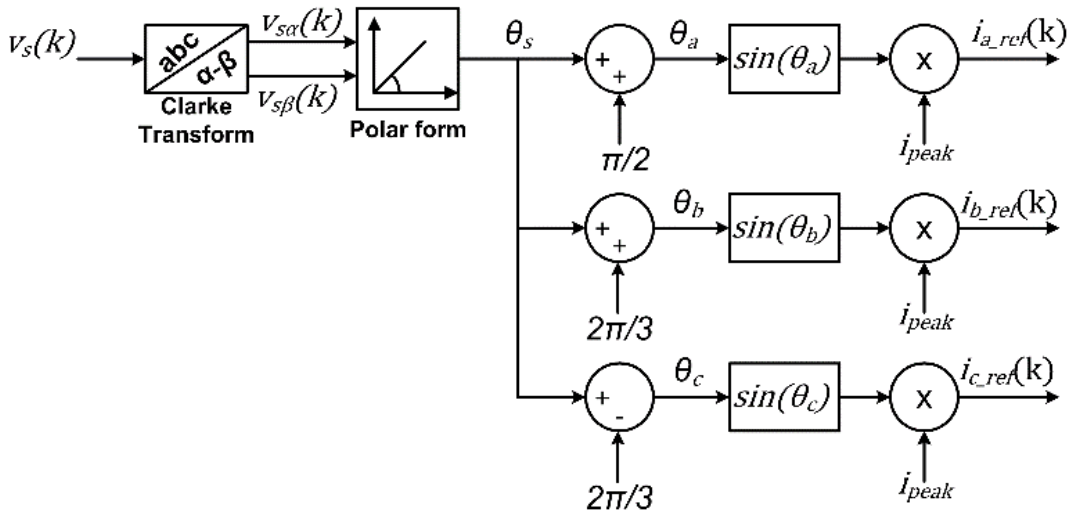

Figure 2.32. Current reference circuit of the MPC controller [29].

The current injected into the grid evaluates the load demand, the redundant delivery to the load (islanded load mode), so the rest inject to the grid.

This work will be the basis of this thesis and will work in two modes (grid-connected mode and stand-alone mode). While connected to a PV-array system, the current injected into the grid will be calculated depending on the power generated in the PV-array system.

2.4. CONCLUSION

What we can conclude from this literature review is that the MPC controller is the most promising method due to of its many good characteristics, including overcoming a number of problems such as:

- The modulation problem as there is no need for a modulation stage in this type of controller.
- Delete delay problems occurring in another controller because the MPC controller being directly implemented in the system.

- The ease of combining with other theories such as Lyapunov or sphere decoding [28][2].

PART 3

INTRODUCTION

This study uses the direct model predictive controller to control a three-phase grid-connected inverter supplied by a PV-Array system. The MPC controls the current injected into the grid by flowing the reference signal, which is constructed by the grid voltage angle. The magnitude of this reference current depends on the power generated by the PV-Array. The optimization of this system depends on the cost function to reduce the tracking error. This work is guided by the previous work [29].

3.1. SYSTEM TOPOLOGIES

3.1.1. The Booster Configuration

Figure 3.1 shows the booster of the system which is used to deduce the maximum power from the PV-Array system depending on Perturb and Observe algorithm. Another booster is used to maintain the inverter DC-voltage input at a constant rate by using an algorithm to maintain the DC-voltage near to the operation voltage, as shown below in Figure 3.1.

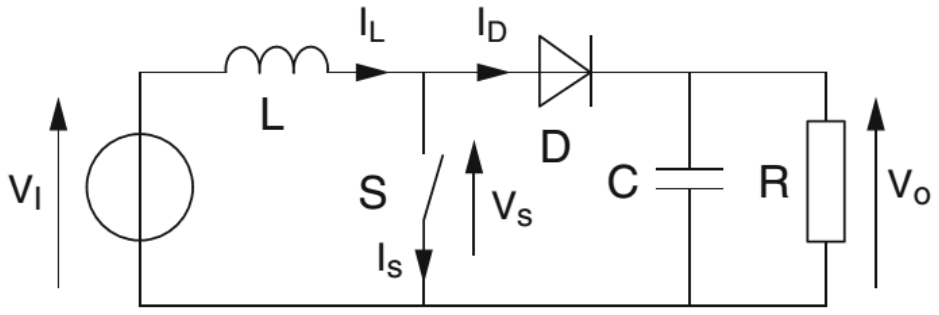

Figure 3.1. PV-array booster configuration [30].

3.1.2. Inverter Configuration

The second stage is the three-phase grid-connected inverter which consists of an LCL filter to suppress occurrences of harmonics due to switching frequencies with the power electronics six drives (MOSFET-diode). This DC supplier is the booster that uses the MPPT algorithm to extract the maximum power from the PV-array system. The function of the MPC controller is to manipulate the driver's states in each leg, which means opening the upper or the lower driver. It is forbidden to open both simultaneously, as opening both causes a short circuit and may cause damage to the drives. The LCL filter is used to connect the system with the grid due to its high harmonic suppression ability. Figure 3.2 shows the construction of the two-level inverter with the LCL filter connected to the grid.

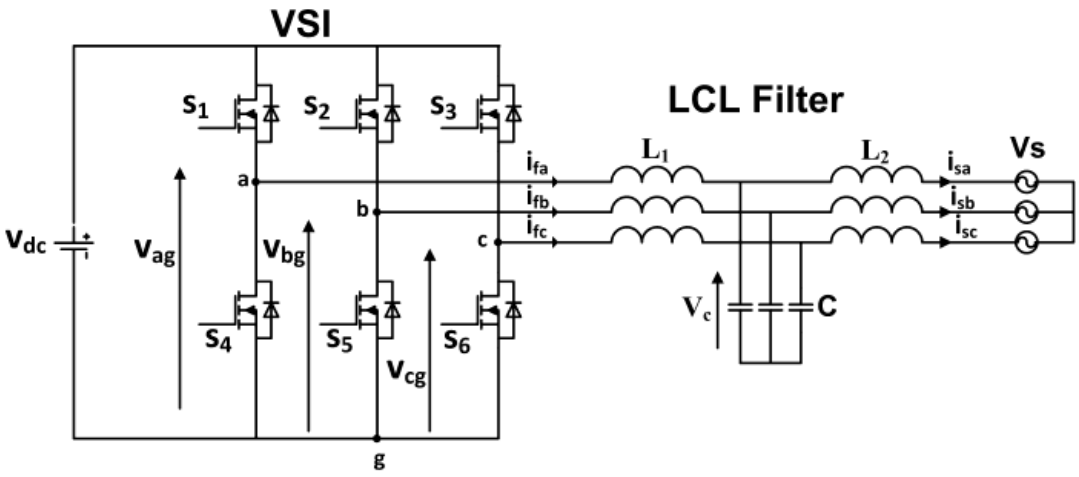

Figure 3.2. Three-phase inverter with LCL filter connected to the grid [29].

3.2. CONSTRAINTS

The legs of the inverters, as shown in Figure 3.2, are connected between the DC voltage source and the LCL filter to the load (the grid). However, at the same time, they can connect the positive and the negative side of the inverter (short circuit), which may cause damage for the drives. Therefore, the first constraints are:

$$ua , ub , uc \epsilon [-1,1] . \quad (3.1)$$

Where ua, ub and uc refere to the switching state in every leg of the inverter.

And u = −1, meaning that the lower driver in the leg of the inverter is closed, and at the same time, the upper driver is open.

3.3. REFERENCE FRAMES

The three-phase system can be transferred into two stationary references, α-β, as shown below ξabc = [ξa ξb ξc] ^{T} to a stationary ξαβ = [ξα ξβ] ^{T} by multiplying the three-phase system by the transformation matrix, thus:

$$\xi\alpha\beta = K\alpha\beta * \xi abc \tag{3.2}$$

$$K\alpha\beta = 2/3\begin{bmatrix} 1 & -1/2 & -1/2 \\ 0 & \sqrt{3/2} & -\sqrt{3/2} \end{bmatrix} \tag{3.3}$$

Where ξ : the vector syombls

$\alpha\beta$: Clark transformation symbols

$K\alpha\beta$: Clark transformation matrix

The opposite can drive it by multiplying it with this matrix:

$$\xi abc = Kabc * \xi\alpha\beta \tag{3.4}$$

$$Kabc = 3/2\begin{bmatrix} 2/3 & 0 \\ -1/3 & \sqrt{3}/3 \\ -1/3 & -\sqrt{3}/3 \end{bmatrix} \tag{3.5}$$

Where $Kabc$: inverse of Clark transformation

In this study, this transformation was used to produce the reference (theta angle) to inject pure energy into the grid (Figure 3.3)

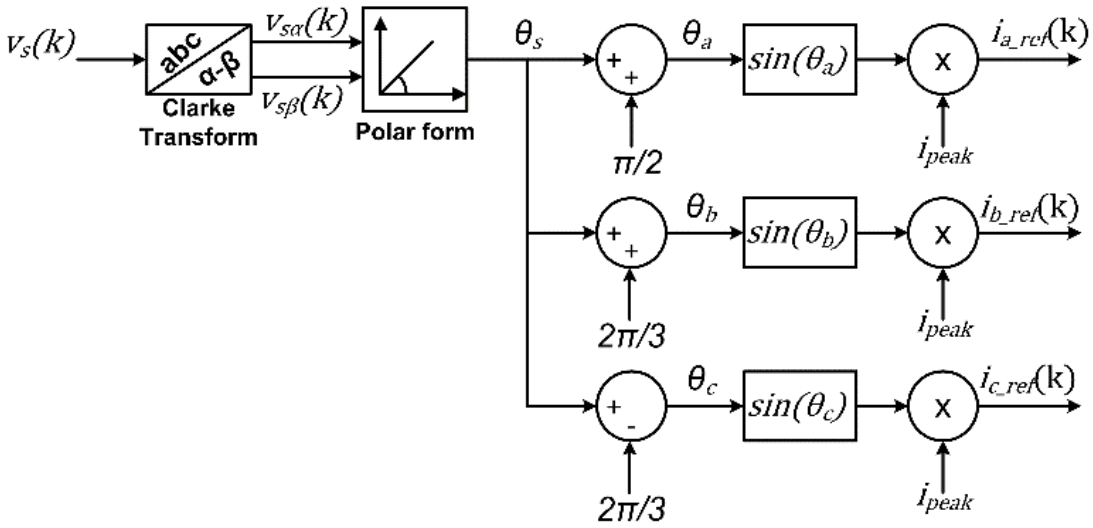

Figure 3.3. Transformation used to produce theta to inject the reference current [29].

3.4. STATE SPACE MODEL

The performance of the model predictive controller depends on the model of the system. Therefore, the inverter case providing the dynamic response for the system depends on the switching stats of the switching driver and the filter connected between the inverter and the grid from a simple view concept. Figure 3.4 illustrates how the state space for the system is extracted.

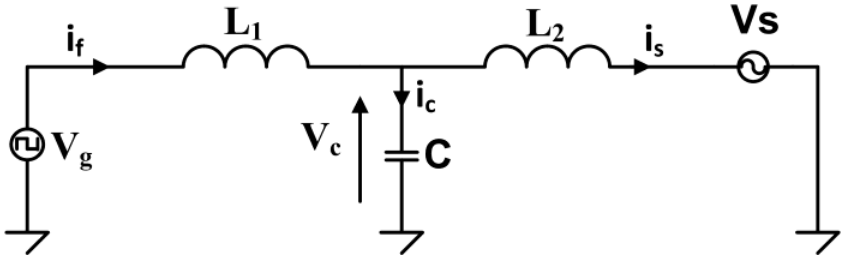

figure 3.4. inverter, filter and grid for a single phase [29].

3.4.1. The State Space Equation

3.4.1.1. General System

$x(k+1) = f(x(k),\ u(k))$ dynamics response (3.6)

$y(k)=g(x(k), u(k))$ static response (3.7)

Where: $x(k+1)$ is the discrete state space of the system

$y(k)$ is the discrete state space of the system

This system or model is not linear, and by using the state space method, the system is converted into a linear system. By discretizing it, the system can be represented as a discrete state space for the LTI system, as in the following equation:

$$\boldsymbol{x}(k+1)n*1 = \boldsymbol{G}\, n*n\,.\,x(k)n*1 + \boldsymbol{H}\, n*m\,.\,\boldsymbol{u}(k)\, m*1 \quad (3.8)$$

$$\boldsymbol{y}(k)r*1 = \boldsymbol{G}\, r*n\,.\,\boldsymbol{x}(k)n*1 + \boldsymbol{D}\, r*m\,.\,\boldsymbol{u}(k)\, m*1 \quad (3.9)$$

where x : the state vector

n : the system order

m : the numbers of inputs

r : the numbers of outputs

G : the state matrix, H : the input matrix, C : the output matrix, and D : the

Direct Link Matrix

Therefore, after the discretization of the system, the ZOH (zero order holder) method is used to implement the controller's output on the design. Figure 3.5 illustrates the concept of the ZOH working principle.

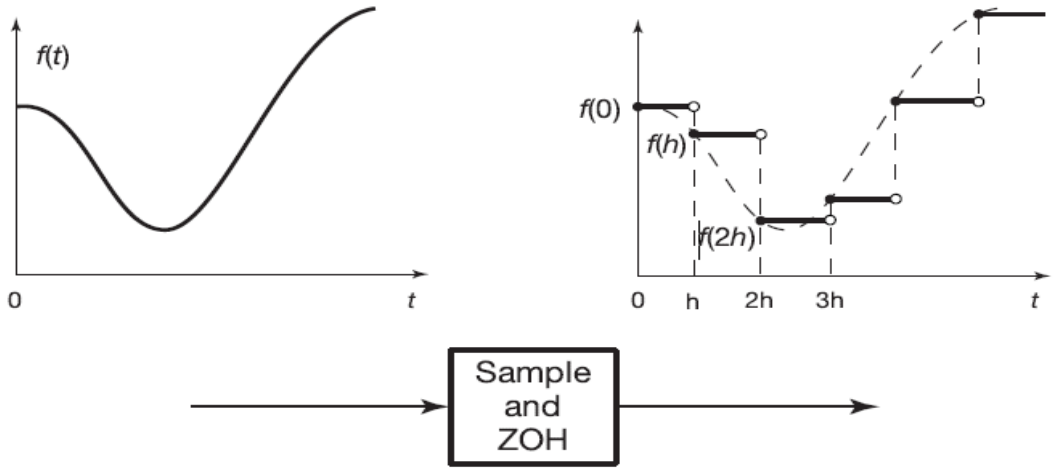

Figure 3.5. Zero order holder (ZOH) basic concept [31].

The signal is entering to the ZOH, then exits to the plant, as shown in Figure 3.6.

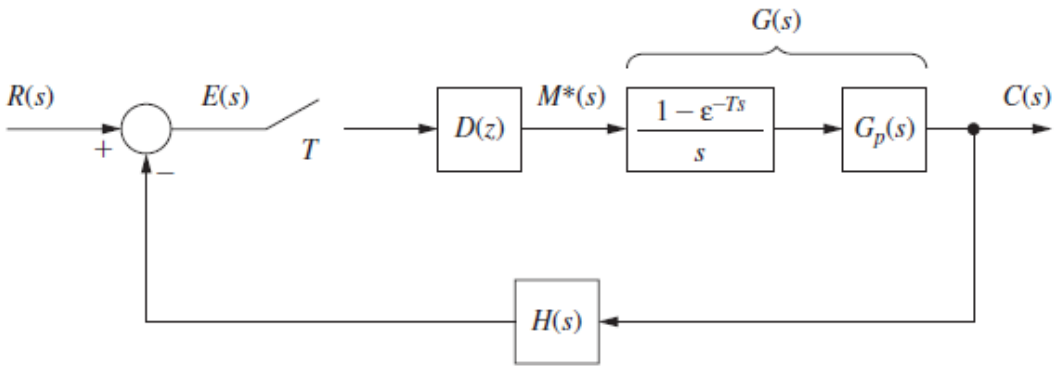

Figure 3.6. Closed loop for ZOH implemented into the system to control the plant (Gp) [32].

Therefore, to deal with the system, we use state space representation, as shown in Figure 3.7.

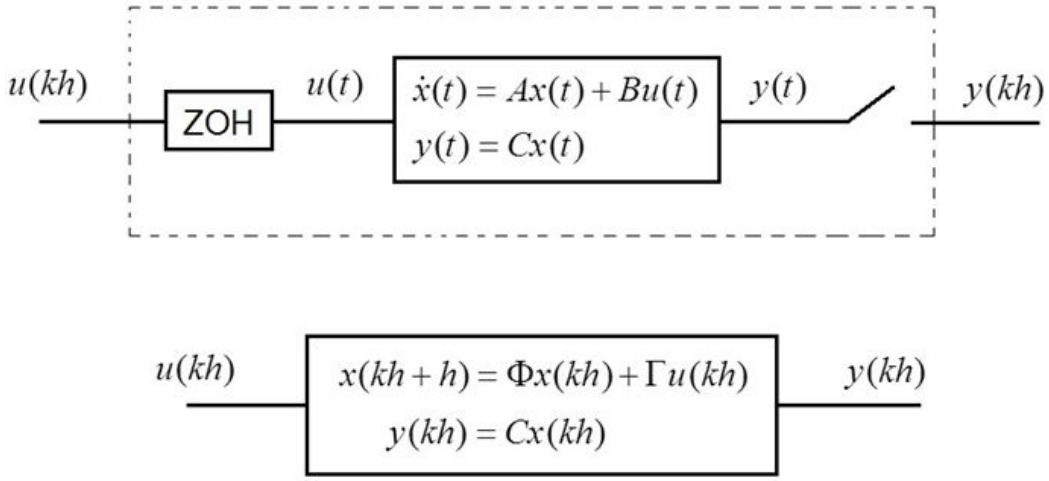

Figure 3.7. Representation of the system by state space and zero-order hold [33].

To find solutions to these equations, the general solution to this equation is found by taking the Laplace to transform thus:

$$\dot{x} = Ax(t) + Bu(t) \tag{3.10}$$

Where x(t) : the state space of the system

u(t) : the system inputs

A and B : the system state matrix

By taking the Laplace transformation,

$$sX(s) - x(0) = AX(s) + BU(s) \tag{3.11}$$

$$(sI - A)X(S) = x(0) + BU(s) \tag{3.12}$$

Where X(s) : the laplace transform of state space matrix

U(s) : the laplace transform of the system input matrix

Then

$$X(s) = (sI - A)^{-1}x(0) + (sI - A)^{-1}B\ U(s) \tag{3.13}$$

Now by taking the Laplace transform

$$x(t) = e^{AT} * x(0) + \int_{\tau}^{t} e^{A(t-\tau)} Bu(\tau) d\tau \quad (3.14)$$

$$\Rightarrow y(t) = C\ e^{AT} x(0) + C\ \int_{\tau=0}^{t} e^{A(t-\tau)}\ B\ u(\tau)\ d\tau \quad (3.15)$$

and after rearranging this equation, the final equation will be

$$x\big((k+1)h\big) = e^{AT} x(kh) + \int_{0}^{h} e^{A\lambda}\ B\ \ d\lambda\ u(kh) \quad (3.16)$$

$$x(k+1)h = \Phi\ x(kh) + \Gamma\ u(kh) \quad (3.17)$$

$$y(kh) = C\ x(kh) \quad (3.18)$$

where $\Phi = e^{Ah}$, and $\Gamma = \int_{0}^{h} e^{A\lambda}\ d\lambda$.

$x(kh)$: discrete state space of the system

$y(kh)$: the discrete output of the system

Depending on Figure 3.3, the state space for the system can be deduced as state space according to the following equations

$$\frac{dif}{dt} = \frac{1}{L1} * (Vg - Vc) \quad (3.19)$$

$$\frac{dis}{dt} = \frac{1}{L2} * (Vc - Vs) \quad (3.20)$$

$$\frac{dVc}{dt} = \frac{1}{C} * (if - is) \quad (3.21)$$

Where Vg : the inverter side voltage

Vc: is the capacitor voltage

Vs: is the grid side voltage

if = filter input current

is = grid injected current

Vc = capacitor voltage

L1, L2 and C are the inductances and capacitances of the LCL filter, respectively.

From these state space equations, the continuous transfer function can be deduced, thus:

$$\begin{bmatrix} dif/dt \\ dis/dt \\ dVc/dt \end{bmatrix} = \begin{bmatrix} 0 & 0 & -1/L1 \\ 0 & 0 & 1/L2 \\ 1/C & -1/C & 0 \end{bmatrix} \begin{bmatrix} if \\ is \\ Vc \end{bmatrix} + \begin{bmatrix} 1/L1 & 0 \\ 0 & -1/L2 \\ 0 & 0 \end{bmatrix} \begin{bmatrix} Vg \\ Vo \end{bmatrix} \quad (3.22)$$

To work with the MPC controller, these state space equations (differential equations) must be transferred to discrete formulas (difference equations) to digitalize it for the microprocessor to deal with it as a digital signal.

Depending on the zero-order holder method, we convert the continuous system equation into a discrete equation:

$$x\big((k+1)h\big) = e^{AT}x(kh) + \int_0^h e^{A\lambda}\ B\ \ d\lambda\, u(kh) \quad (3.23)$$

where A = $\begin{bmatrix} 0 & 0 & -1/L1 \\ 0 & 0 & 1/L2 \\ 1/C & -1/C & 0 \end{bmatrix}$ and B = $\begin{bmatrix} 1/L1 & 0 \\ 0 & -1/L2 \\ 0 & 0 \end{bmatrix}$

With this method, we convert the system into a discrete system and apply the following output result:

$$y(kh) = C\ x(kh)$$

Applying to the cost function, the discretization of this continuous system is done on MATLAB order c2d depending on the zero-order holder method to implement it next in the cost function [33].

3.5. THE COST FUNCTION

The main goal of the cost function is to minimize the output error with respect to the reference produced by outer control loop or circuit, such as the maximum power produced by the PV array.

According to this equation

$g = |\, imeas^2 - iref^2|$ (3.24)

Where $imeas$: the outpue measured current

Iref : the reference measured current

the three phase system can be compared with an alpha-beta reference, as in the following equation [34]:

$$g = |i\alpha^p(k+1) - i\alpha(k+1)ref| + |i\beta^p(k+1) - i\beta(k+1)ref| \quad (3.25)$$

Where : $i\alpha(k+1)ref$ and $i\beta(k+1)$ref is the reference current in Clarke transformation method

: $i\alpha^p(k+1)$ and $i\beta^p(k+1)$ is the predictive current in Clarke transformation method

In this study, the direct comparison without using alpha-beta transform is used.

$$g = |ia^p(k+1) - ia(k+1)ref| + |ib^p(k+1) - ib(k+1)ref| + |ic^p(k+1) - ic(k+1)ref| \quad (3.26)$$

The working principle for the cost function in the inverter is illustrated in Figure 3.8.

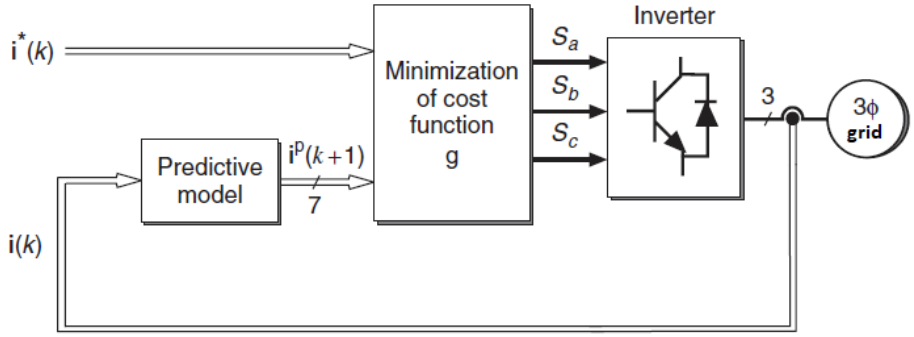

Figure 3.8. Predictive current control block diagram [34].

The predictive algorithm depends on the model discretization of the inverter with the LCL to reduce the tracking error. The current control algorithm depends on these four steps:

- The current reference values are obtained from the outer control reference and synchronize with the grid voltage to inject pure power into the grid.
- The system model is used to predict the next switching combination for each voltage vector to track the reference current.
- To reduce error, the cost function evaluates the error for each switching combination or voltage vector.
- The switching combination (switching state) or voltage vector that reduces the output current error is selected.

Figure 3.9 illustrates the switching combination.

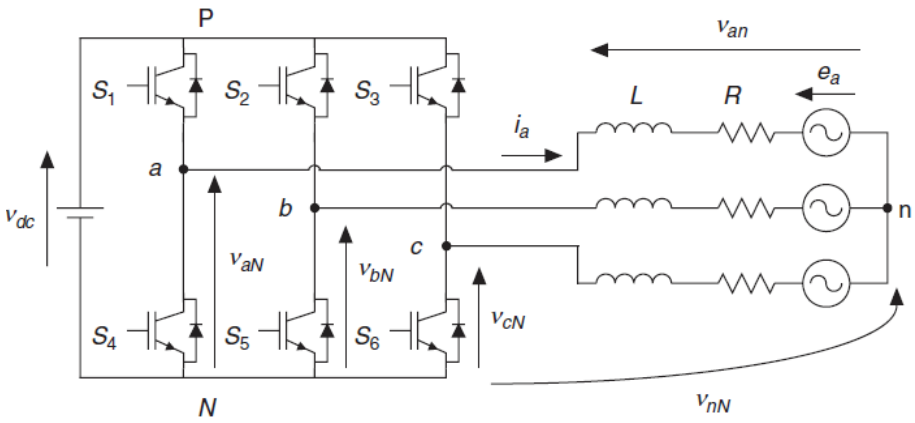

Figure 3.9. Voltage source inverter [34].

As shown in Figure 3.8, the inverter is combined from three legs and a three-phase, two-level inverter controls the filter input voltage by controlling the DC voltage source according to its driver combination or switching signals Sa, Sb and Sc.

These are defined thus:

$$Sa = \begin{cases} 1 \; if \; S1 \; is \; on \; and \; S4 \; is \; off \\ 0 \; if \; S1 \; is \; on \; and \; S4 \; is \; on \end{cases}$$

$$Sb = \begin{cases} 1 \; if \; S2 \; is \; on \; and \; S5 \; is \; off \\ 0 \; if \; S2 \; is \; on \; and \; S5 \; is \; on \end{cases}$$

$$Sc = \begin{cases} 1 \; if \; S3 \; is \; on \; and \; S6 \; is \; off \\ 0 \; if \; S3 \; is \; on \; and \; S6 \; is \; on \end{cases}$$

These switching signals define the output (drive output) into the filter according to the following:

$$VaN = Sa * Vdc$$

$$VbN = Sb * Vdc$$

$$VcN = Sc * Vdc$$

where *Vdc* is the source voltage and VaN, VbN, VcN are the phases of the natural (N) voltage of the inverter.

By considering unity vector $a = e^{j*2\,\pi/3} = \frac{-1}{2} + j\frac{\sqrt{3}}{2}$, which represents the phase difference (displacement) between phases, the output of the drive will be

$$V = 2/3(Van + aVbn + a^2Vcn)$$

Thus, the voltage vector is produced according to the switching states as follows:

(Sa, Sb, Sc) = (0,0,0) generates the output voltage $V = \left(\frac{2}{3}\right)(\,0 + a * 0 + a^2 * 0) = 0.$ Another example where the switching states are (1,0,0), $V = \left(\frac{2}{3}\right)(\,Vdc + a * 0 + a^2 * 0) = \frac{2}{3}Vdc$ and so on. Therefore, the switching states will be as in the table below.

Table 3.1. Switching states and voltage vectors [34].

Sa	**Sb**	**Sc**	**Voltage vector V**
0	0	0	V0=0
1	0	0	V1=2/3 *Vdc
1	1	0	$V2 = \frac{1}{3}Vdc + j\frac{\sqrt{3}}{3}Vdc$
0	1	0	$V3 = \frac{1}{3}Vdc + j\frac{\sqrt{3}}{3}Vdc$
0	1	1	$V4 = -\frac{2}{3}Vdc$
0	0	1	$V5 = -\frac{1}{3}Vdc - j\frac{\sqrt{3}}{3}Vdc$
1	0	1	$V6 = \frac{1}{3}Vdc - j\frac{\sqrt{3}}{3}Vdc$
1	1	1	$V3 = 0$

Figure 3.10 shows the voltage vector in the complex plane.

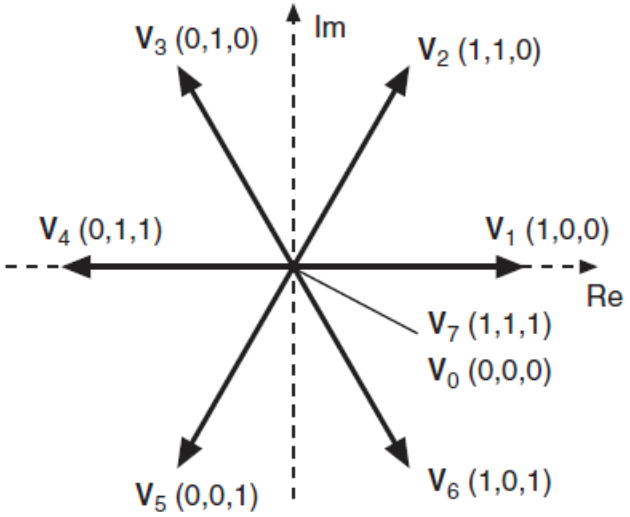

Figure 3.10. Voltage vector of the three-phase inverter [34].

3.6. WORKING PRINCIPLE

To illustrate how the predictive model controller works, Figure 3.11 gives a detailed example of the MPC strategy. This figure explains how the cost function works by comparing the error between the reference and the measured signal and selecting the voltage vector, which gives the minimum error of the output current.

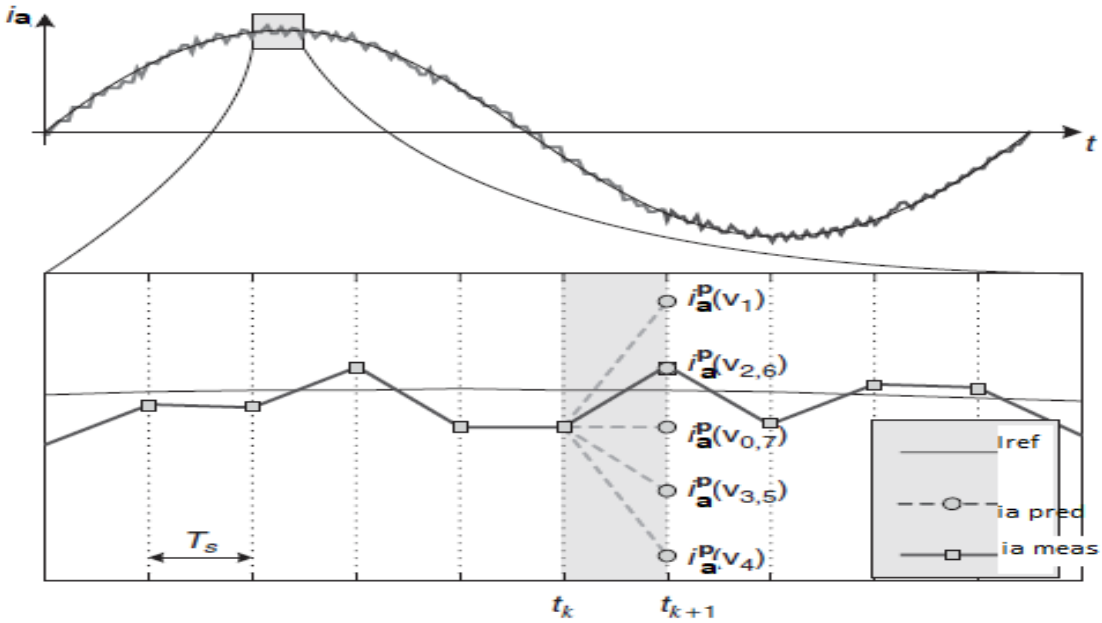

Figure 3.11. Working principle of the MPC controller [34].

3.7. SUMMARY

In this chapter, a three-phase grid-connected current control design is illustrated using the MPC controller (FCS) with the eight possible switchings for the three-leg inverter. Selecting an MPC controller that minimizes the tracking error of the reference, and the state space of the system derived to capture the dynamic of the system by using the FCS technique (only eight switchings are possible in this model) will find which switching state is the nearest for the reference to produce the lowest possible error. The reference current is produced by using the grid voltage's polar method and calculating the power produced by the PV array to find the reference current magnitude injected into the grid with the unity power factor.

PART 4

IMPLEMENTATION AND RESULTS

4.1. INTRODUCTION

In this chapter, the implementation of the MPC controller will reveal advantages such as simplicity and high-speed dynamic response by demonstrating the result of the MATLAB simulation and how it works in two conditions, which are the grid-connected mode and the stand-alone mode, so simulation results will be presented.

4.2. SIMULATION DESIGN

4.2.1. Model Predictive Control

The basic concept of the MPC controller is presented in Figure 1, which illustrates its dependence on the finite step set, which is three-phase and a full bridge inverter with eight switching states. The reference signal in this controller was deduced using the alpha-beta and polar transformer and implemented into the algorithm to find the optimized solution, as mentioned in Chapter 3.

The MPC algorithm works in two modes, the grid-connected mode and the stand-alone mode using *if-else* as a condition for grid states.

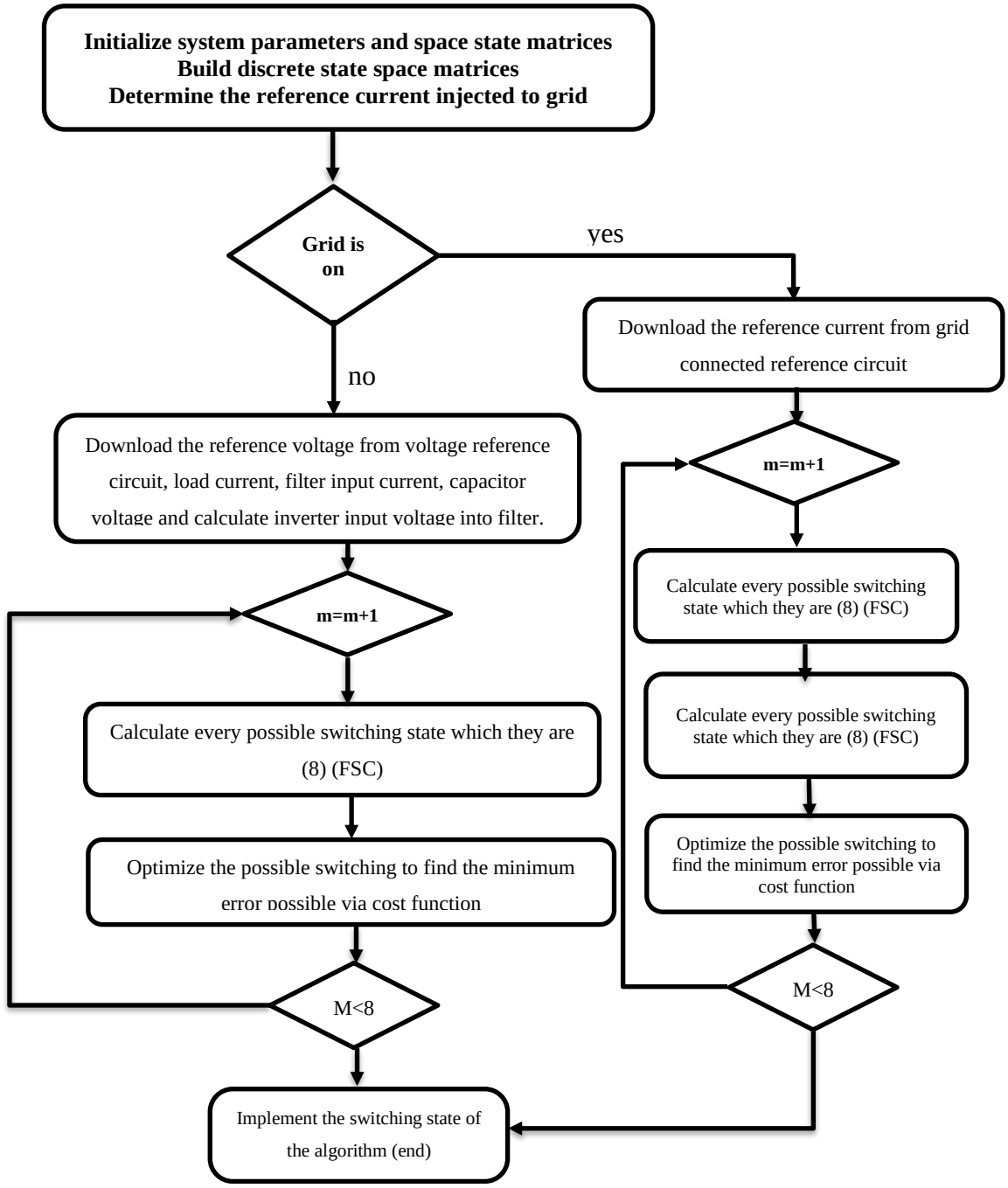

Figure 4.1. Basic concept of the MPC controller algorithm for Finite Set Control (FSC).

4.2.2. System Parameters

Two boosters supply the system such that the first is connected with the PV-Array system and the second is associated with the battery system to maintain a fixed voltage for the inverter input. The first booster (the PV-array booster) is controlled by maximum power point tracking (MPPT) via the Perturb and Observe algorithm to

deduce the maximum power from the solar cells, while the function of the second booster is to maintain the voltage supplied to the inverter at a fixed value even when the load is very high, thereby ensuring system stability.

The grid's frequency is 50 Hz and the voltage is 400 volts on average (line to line). The system has a fast dynamic response to both changing frequency and the voltage values.

The output power of the system is 250 KVA, so the output current will be 360 A.

4.2.2.1.The Boosters

Figure 4.2 shows the PV-Array characteristic.

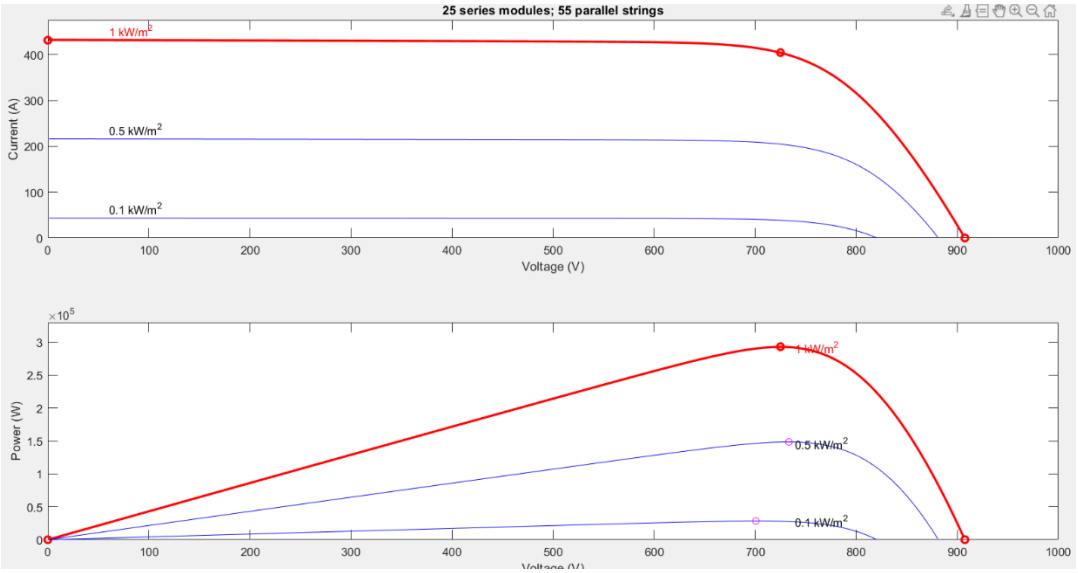

Figure 4.2. PV-Array characteristic.

The first capacitor is 1000 mF which is connected in parallel with the PV-array to maintain the output voltage, while the inductance is approximately 100 micro-H with 1 mΩ resistance. The second booster connected to the battery system has the same inductance value as the two boosters connected with the same capacitor, which is 1000 mF.

The impact of the voltage booster is that it makes the voltage closer to the reference voltage and simultaneously connects the system with ESS to ensure its stability when a high load connects to the system also used to store extra energy produces by the PV-Array system figure (4.3) shows the effect of connected the voltage regulator booster.

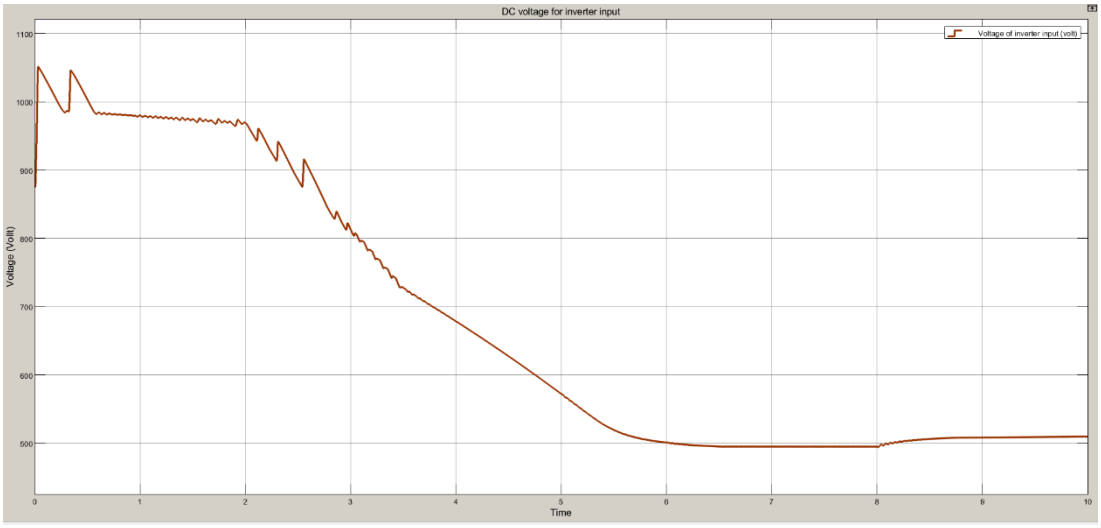

(a) Without voltage regulator booster.

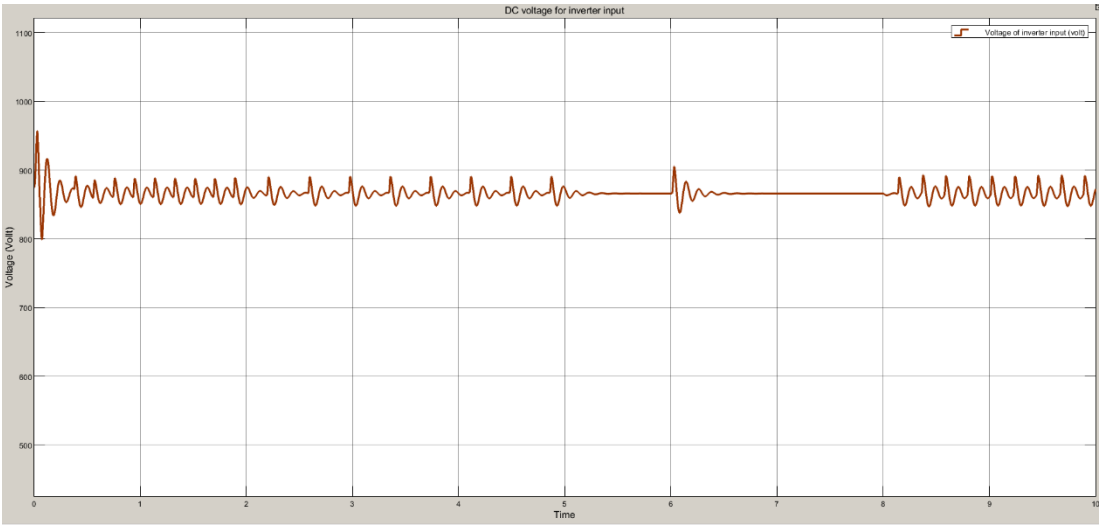

(b) With voltage regulator booster.

Figure 4.3. Effect of connecting the voltage booster.

4.2.2.2. LCL Filter

There are three types of filter used to connect the inverter:

- The L filter
- The LC filter
- The LCL filter

The L filter was widespread until 1992, when the IEEE standards rose. In order to meet this standard, the L filter had to be bulky and expensive. Moreover, the LC filter inductor did not change much, so the LCL filter became an attractive option. The advantage of the LCL filter is that it has high attenuation compared with the L filter. The disadvantage, however, was that the LCL has resonant frequency (see Figure 4.4).

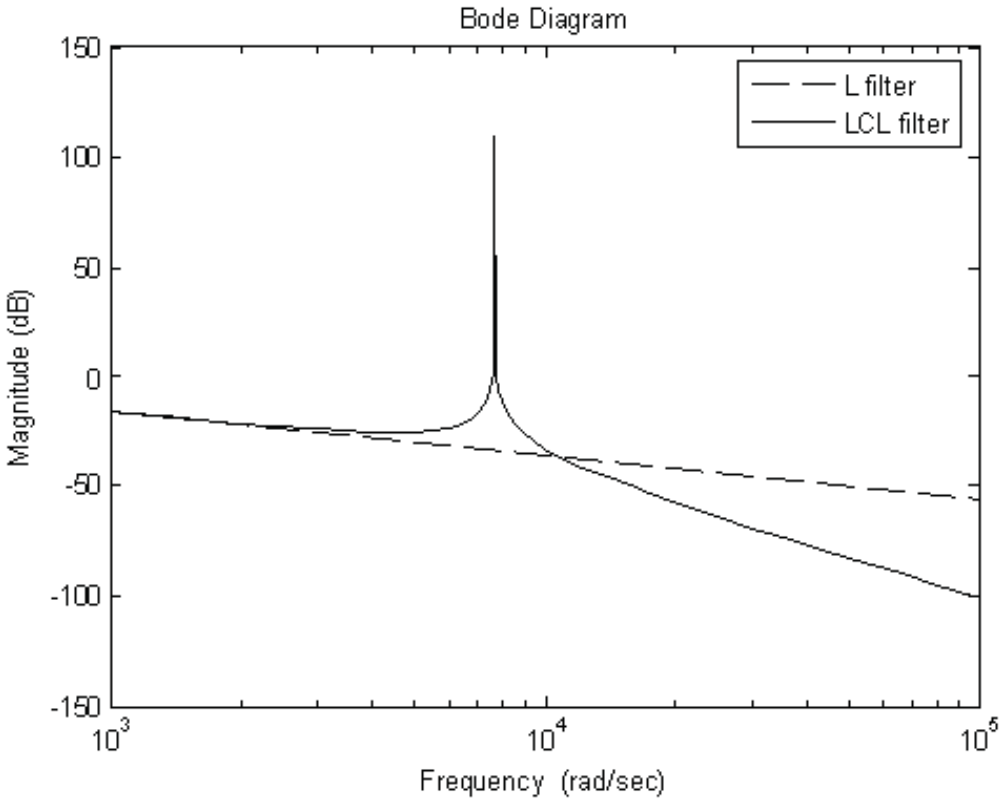

Figure 4.4. Attenuation characteristic of the LCL and L filters [35].

Therefore, care must be given not to feed this resonant frequency with energy. The working principal harmonics will pass through the capacitor at high frequency because it is followed by inductance with very high impedance at a high frequency.

There are two resonant frequencies, as in the following figure.

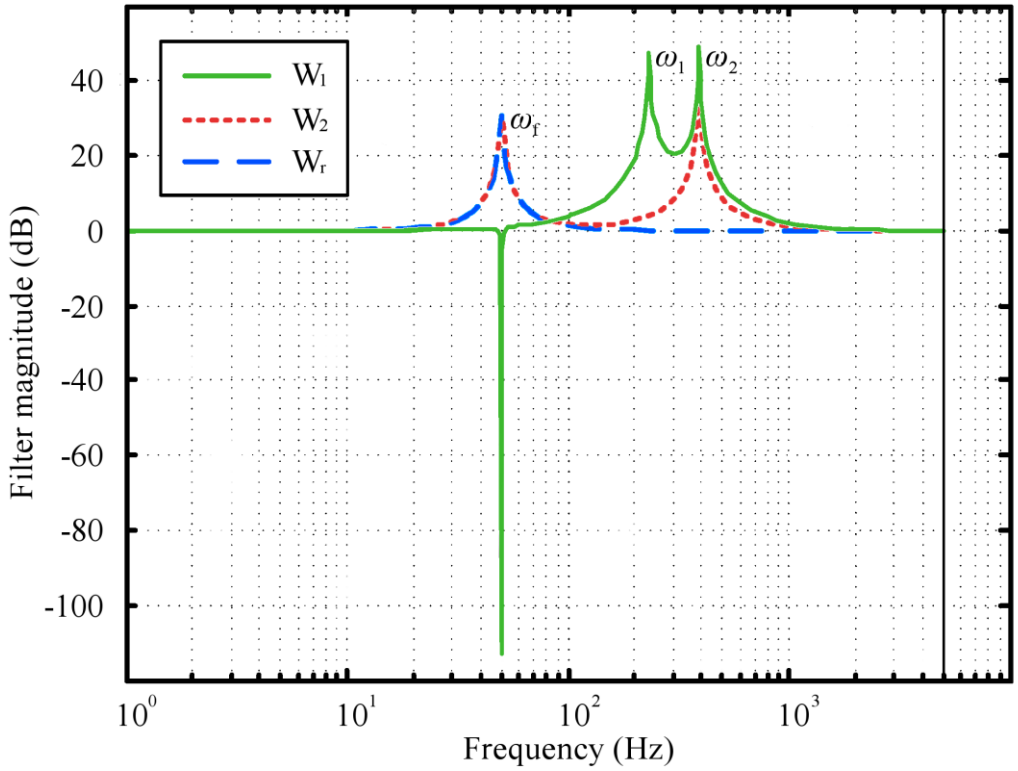

Figure 4.5. Resonant frequencies for the LCL filter [2].

LCL Filter Parameters

Table 4.1. LCL Filter Parameters.

Parameters		
Nominal grid voltage amplitude	$231\sqrt{2}$	volt
Maximum current amplitude	360	Ampere
Inverter side inductance (L1)	0.27	mH
Grid side inductance (L2)	0.2	mH
Filter capacitor	200	µF

The filter parameters are calculated depending on the voltage drop on the inductance most not exceeding 10% of the system's nominal voltage, while the capacitor value is selected to contain approximately 5% of the system's output power as a VAR value.

4.3. REFERENCE CONTROL CIRCUITS

In this work, we have two reference circuits, the first of which is grid-connected (as mentioned in Chapter 3). The other is a stand-alone reference which is merely a three-phase signal with a deference phase of 120°.

The algorithm, in this case, will be for the voltage controller, not for the current controller, because the grid will be cut off in a stand-alone state.

4.4. SIMULATION RESULT

The main objective of this system is to convert the irradiation energy into electrical energy and inject it into the grid as pure energy (unity power factor), as shown in Figure (4.6).

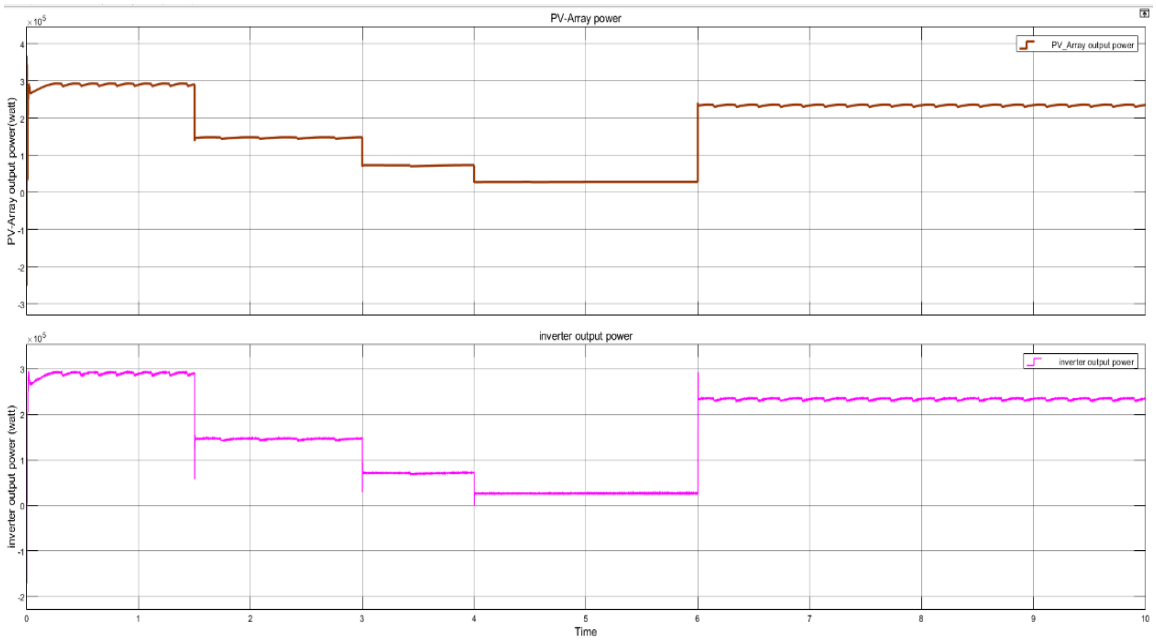

Figure 4.6. PV-Array power versus electrical power injected into the grid.

Figure 4.7 shows the output voltage of the PV-Array into the inverter with and without voltage regulation booster.

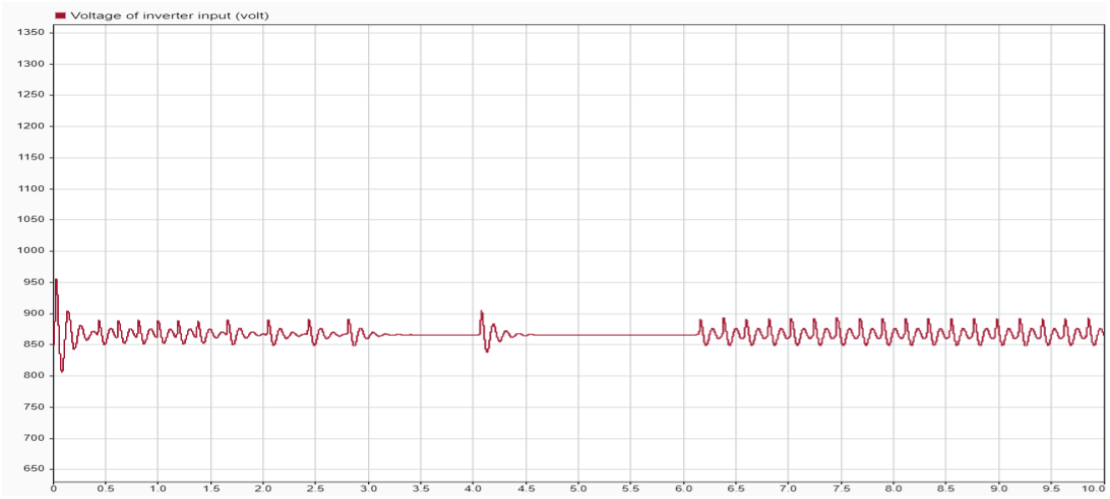

(a)

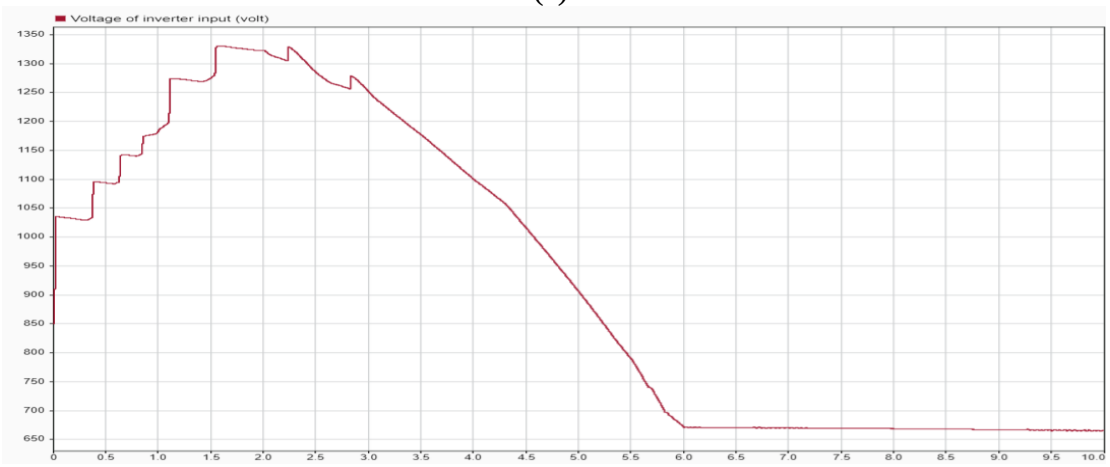

(b)

Figure 4.7. The inverter voltage input (a) with voltage regulator booster and (b) without voltage regulator booster.

The system has a very fast dynamic response to the change in the grid voltage magnitude and low frequency harmonic, which meets the standards of the IEEE, figure (4.8) shows the dynamic respond of the system to change in PV-Array power.

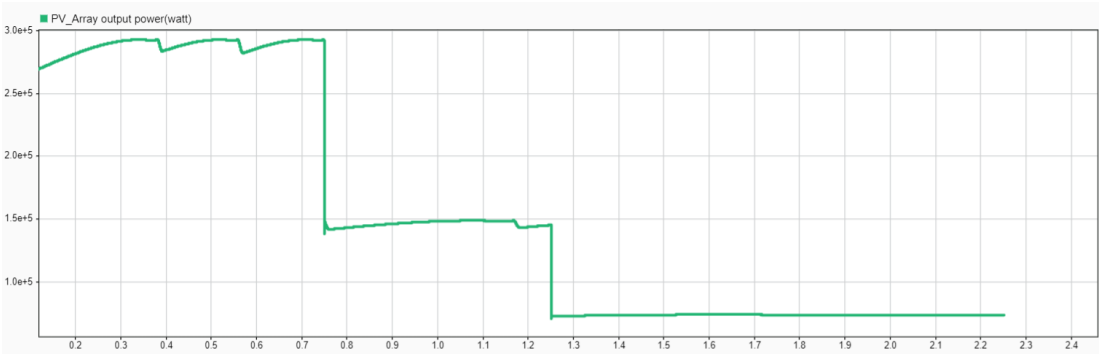

(a)

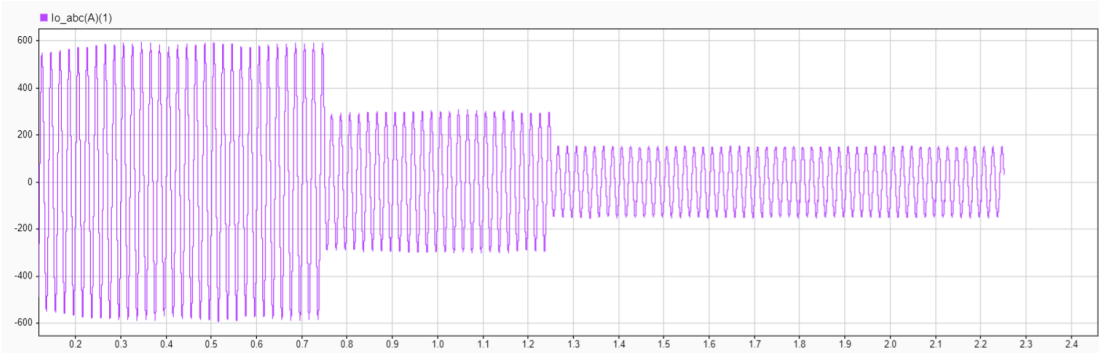

(b)

Figure 4.8. (a) Inverter output power (b) inverter injected current into the grid.

As shown in Figure 4.9, the dynamic response to the change to the generated power is very fast, and the total harmonic distortion (THD) as shown in the figure below.

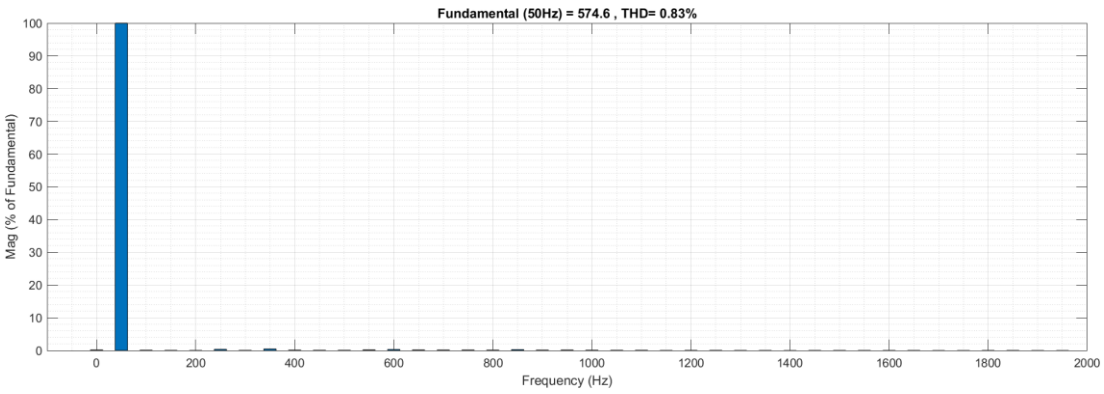

Figure 4.9. THD of the system is approximately 0.83%, which meets IEEE standards.

4.5. COMPARING WITH PREVIOUS STUDIES

When we are comparing with the other controller, such as the PID controller, we find that the MPC controller is better.

For the total harmonic distortion, as shown in Figure 4.10 a, THD = 0.83 for the MPC controller.

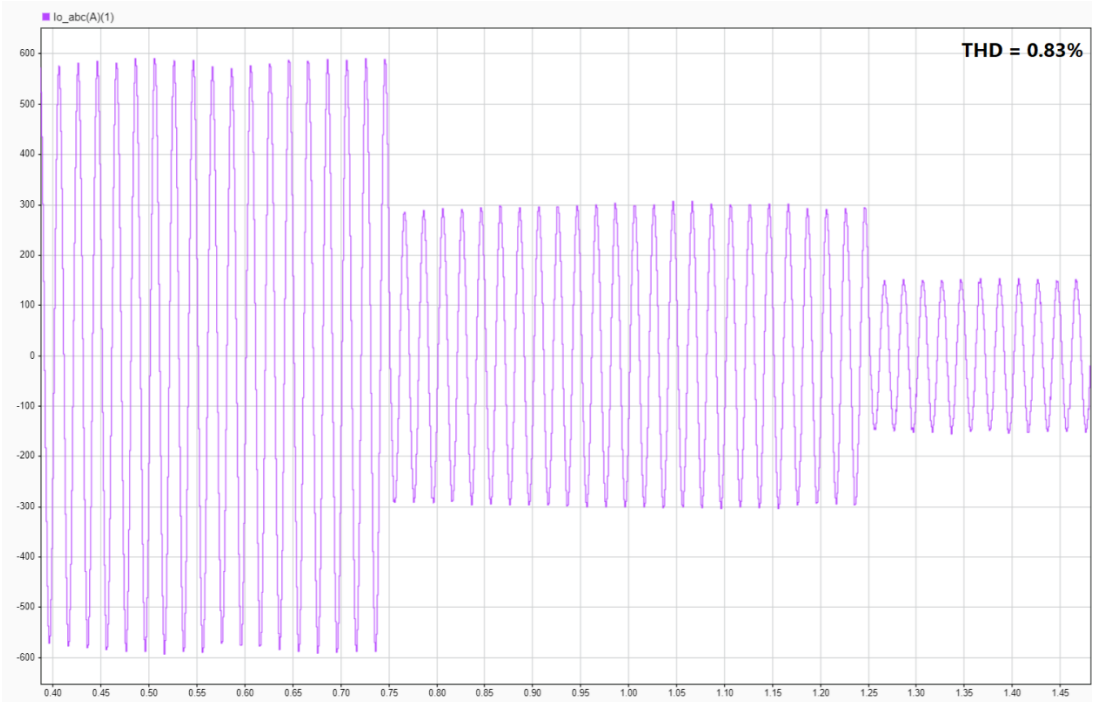

Figure 4.10. THD for MPC controller.

4.6. FUTURE WORK

The main disadvantage of the MPC controller is the huge amount of calculation for the FSC-finite set control, the calculation that is the most performed for each one to find the optimized switching to produce the lowest error. This is for one step ahead predictive or the receding horizon principle. However, the calculation will grow exponentially if the control horizon is expanding to more than one step. Therefore, reducing the amount of computation is very important to overcome this problem to produce controller work with long horizon. This leads to a reduction in the switching frequency, which in turn provides more than one advantage:

- It reduces the switching effort on the inverter drives, which means a longer life span for the inverter.
- We can reduce switching losses.
- We can reduce harmonics, especially high-frequency harmonics, due to lower switching frequency.

PART 5

CONCLUSION

The environmental problem presented a challenge that makes renewable energy an attractive replacement for fossil fuels due to the greenhouse gas emissions of CO_2, CH_4, etc. For this reason, we have prepared the PV-Array with the MPPT algorithm to produce the maximum electric power from the solar cells and merged it with the MPC for the LCL filter to control the power injected into the grid, which is the purpose of this study.

The representations of this work are based on the PV-Array with two boosters. The MPPT controller controls the first, while the second booster is controlled by the algorithm to maintain the inverter input voltage around a fixed range and to maintain system stability through high load fluctuation. The MPC algorithm controls the inverter to control the current injected into the grid, and the magnitude and phase of this current is deduced by the outer control loop to calculate its magnitude, frequency and phase. This current is injected through the LCL filter due to its high harmonic attenuation characteristics.

The key to any electrical system is the control techniques, which is the main target of this study. The MPC controller proved the strength of performance and the strictness of the constraints possessed by this type of control. From one perspective, such as accuracy, we do not need to add stages to linearize the nonlinear system (as in the case of the PID and PR controller) such as the PWM, which deletes the delay time. This may occur due to this stage, reduce the cost of the system and increase its reliability. There is a very fast dynamic response and it is able to combine with many control theories, including Lyapunov theory or sphere decoding. However, it requires many calculations for accurate representation of the system model, a wide operating frequency range and sensitivity with inaccurate parameters of the system.

The challenges of this study are to represent the system, which is the inverter switching drives and their accurate representation, the design the LCL filter, and overcoming the resonant frequencies of the LCL filter, which is the innovation of this work.

Future work can focus on reducing the calculation burden performed by the algorithm, attempting to apply the long horizon method while reducing the calculations needed to achieve this long horizon predictive technique so as to accomplish lower switching frequencies, which in turn reduces harmonics and the tension on converter drives, thereby leading to longer life spans and better reliability.

REFERENCES

[1] B. K. Bose, "Global energy scenario and impact of power electronics in 21st century," *IEEE Transactions on Industrial Electronics,* vol. 60, no. 7, pp. 2638-2651, 2012.

[2] J. M. C. Geldenhuys, "Model predictive control of a grid-connected converter With LCL-filter," Stellenbosch: Stellenbosch University, 2018.

[3] H. Ritchie and M. Roser, "CO_2 and greenhouse gas emissions," *Our world in data,* 2020.

[4] A. Rashedi, T. Khanam, and M. Jonkman, "On reduced consumption of fossil fuels in 2020 and its consequences in global environment and exergy demand," *Energies,* vol. 13, no. 22, p. 6048, 2020.

[5] Q. Zhong, M. Malinowski, B. Francois, and E. Romero-Cadaval, "Grid-connected photovoltaic generation plants as alternative energy sources," *IEEE Industrial Electronics Magazine,* vol. 9, no. 1, pp. 18-32, 2015.

[6] R. Luhtala, "Real-Time Identification and Adaptive Control of Grid-Connected Three-Phase Inverters," 2020.

[7] M. A. W. Begh, "Closed Loop Current Control of a Grid Connected Transformerless Flying Capacitor Inverter," 2018.

[8] A. Moghadasi, A. Sargolzaei, A. Anzalchi, M. Moghaddami, A. Khalilnejad, and A. Sarwat, "A model predictive power control approach for a three-phase single-stage grid-tied PV module-integrated converter," *IEEE Transactions on Industry Applications,* vol. 54, no. 2, pp. 1823-1831, 2017.

[9] T. D. C. Busarello, J. A. Pomilio, and M. G. Simoes, "Design procedure for a digital proportional-resonant current controller in a grid connected inverter," in *2018 IEEE 4th Southern Power Electronics Conference (SPEC)*, 2018: IEEE, pp. 1-8.

[10] S. Bacha, I. Munteanu, and A. I. Bratcu, "Power electronic converters modeling and control," *Advanced textbooks in control and signal processing,* vol. 454, no. 454, 2014.

[11] C. E. Garcia, D. M. Prett, and M. Morari, "Model predictive control: Theory and practice—A survey," *Automatica,* vol. 25, no. 3, pp. 335-348, 1989.

[12] M. S. R. Nandurkar and M. M. Rajeev, "Design and Simulation of three phase Inverter for grid connected Photovoltic systems," *Power,* vol. 10, p. 30KW, 2012.

[13] M. J. Mnati, D. V. Bozalakov, and A. Van den Bossche, "PID Control of a Three Phase Photovoltaic Inverter Tied to a Grid Based on a 120-Degree Bus Clamp PWM," *IFAC-PapersOnLine*, vol. 51, no. 4, pp. 388-393, 2018.

[14] R. A. Kadhim, "Design and simulation of closed loop proportional integral (PI) controlled boost converter and 3-phase inverter for photovoltaic (PV) applications," *Al-Khwarizmi Engineering Journal*, vol. 15, no. 1, pp. 10-22, 2019.

[15] M. Louzazni and E. Aroudam, "Control and stabilization of three-phase grid connected photovoltaics using PID-Fuzzy logic," in *2014 IEEE international conference on intelligent energy and power systems (IEPS)*, 2014: IEEE, pp. 279-284.

[16] J. S. Dohler, P. M. de Almeida, and J. G. de Oliveira, "Droop control for power sharing and voltage and frequency regulation in parallel distributed generations on ac microgrid," in *2018 13th IEEE International Conference on Industry Applications (INDUSCON)*, 2018: IEEE, pp. 1-6.

[17] J. M. Geldenhuys, H. du Toit Mouton, A. Rix, and T. Geyer, "Model predictive current control of a grid connected converter with LCL-filter," in *2016 IEEE 17th Workshop on Control and Modeling for Power Electronics (COMPEL)*, 2016: IEEE, pp. 1-6.

[18] I. M. Syed and K. Raahemifar, "Model Predictive Control of Three Phase Inverter for PV Systems," *International Journal of Energy and Power Engineering*, vol. 9, no. 10, pp. 1188-1193, 2015.

[19] N. Güler and E. Irmak, "MPPT Based Model Predictive Control of Grid Connected Inverter for PV Systems," in *2019 8th International Conference on Renewable Energy Research and Applications (ICRERA)*, 2019: IEEE, pp. 982-986.

[20] Y. Zhao, A. An, Y. Xu, Q. Wang, and M. Wang, "Model predictive control of grid-connected PV power generation system considering optimal MPPT control of PV modules," *Protection and Control of Modern Power Systems*, vol. 6, no. 1, pp. 1-12, 2021.

[21] H. Laabidi, H. Jouini, and A. Mami, "A Control Strategies of PV System based on VOC, SMC and MPC Algorithms," *Indian Journal of Science and Technology*, vol. 12, p. 31, 2019.

[22] H. Gholami-Khesht, P. Davari, and F. Blaabjerg, "An Adaptive Model Predictive Voltage Control for LC-Filtered Voltage Source Inverters," *Applied Sciences*, vol. 11, no. 2, p. 704, 2021.

[23] R. Guzman, L. G. de Vicuña, A. Camacho, J. Miret, and J. M. Rey, "Receding-horizon model-predictive control for a three-phase VSI with an LCL filter," *IEEE Transactions on Industrial Electronics*, vol. 66, no. 9, pp. 6671-6680, 2018.

[24] N. N. Nam, M. Choi, and Y. I. Lee, "Model Predictive Control of a Grid-Connected Inverter with LCL Filter using Robust Disturbance Observer," *IFAC-PapersOnLine*, vol. 52, no. 4, pp. 135-140, 2019.

[25] T.-L. L. Quang-Tho Tran*, Huu-Lam Ho, Phu-Cuong Nguyen, Quang-Hieu and a. V.-H. T. Nguyen, "Model Predictive Control for Three-phase Grid-Connected Inverters," *International Journal of Advanced Engineering, Management and Science*, 2021, doi: 10.22161/ijaems.

[26] N. Panten, N. Hoffmann, and F. W. Fuchs, "Finite control set model predictive current control for grid-connected voltage-source converters with LCL filters: A study based on different state feedbacks," *IEEE Transactions on Power Electronics*, vol. 31, no. 7, pp. 5189-5200, 2015.

[27] D. K. Yoo, L. Wang, E. Rogers, and W. Paszke, "Model predictive control of three phase voltage source converters with an LCL filter," in *2014 IEEE 23rd International Symposium on Industrial Electronics (ISIE)*, 2014: IEEE, pp. 562-567.

[28] S. Golzari, F. Rashidi, and H. F. Farahani, "A Lyapunov function based model predictive control for three phase grid connected photovoltaic converters," *Solar Energy*, vol. 181, pp. 222-233, 2019.

[29] O. Gulbudak and M. Gokdag, "Predictive Current Control Method with State Observer for Grid-Connected Inverter Equipped with LCL-Filter," in *2021 IEEE 2nd International Conference on Smart Technologies for Power, Energy and Control (STPEC)*, 2021: IEEE, pp. 1-6.

[30] R. R. Sankar, S. J. Kumar, and K. Deepika, "Model Predictive Current Control of Grid Connected PV Systems," *Indonesian Journal of Electrical Engineering and Computer Science*, vol. 2, no. 2, pp. 285-296, 2016.

[31] S. H. Zak, "An Introduction to Model-Based Predictive Control (MPC)," *lecture notes on ECE680, Purdue University*, 2017.

[32] A. Chakrabortty, H. T. Nagle, and C. L. Phillips, "Digital Control System Analysis & Design: Global Edition," ed: Pearson Education, 2015.

[33] https://slideplayer.com/slide/9548170/. "discretization of continuous_time state space models." (accessed.

[34] J. Rodriguez and P. Cortes, *Predictive control of power converters and electrical drives*. John Wiley & Sons, 2012.

[35] F. Liu, X. Zha, Y. Zhou, and S. Duan, "Design and research on parameter of LCL filter in three-phase grid-connected inverter," in *2009 IEEE 6th International Power Electronics and Motion Control Conference*, 2009: IEEE, pp. 2174-2177.

[36] R. Errouissi, A. Al-Durra, and S. Muyeen, "Offset-free feedback linearisation control of a three-phase grid-connected photovoltaic system," *IET Power Electronics*, vol. 9, no. 9, pp. 1933-1942, 2016.

RESUME

My name is Aadil Salam Ahmed ABUMELH I live in Iraq, Babel, Hillah. I graduated from university of Babylon in the academic year (2003-2004) first attempt. I am working as senior engineer in the Iraqi ministry of electricity.